Precambrian Research 407 (2024) 107407

Contents lists available at ScienceDirect

Precambrian Research

journal homepage: www.elsevier.com/locate/precamres

50th Anniversary Invited Review

On the origin of Archaean TTGs by migmatization of mantle plume-related metabasalts: Insights from the Lake Inari terrain, Arctic Fennoscandia

Jaana Halla [a,*], Kumar Batuk Joshi [b], Arto Luttinen [a], Esa Heilimo [c], Matti Kurhila [d]

[a] Geosciences Unit, Finnish Museum of Natural History, University of Helsinki, Finland
[b] Solid Earth Research Group, National Centre for Earth Science Studies, India
[c] Department of Geography and Geology, University of Turku, Finland
[d] Geological Survey of Finland, Finland

ARTICLE INFO

Keywords:
Archaean
Tonalite-trondhjemite-granodiorite
Metabasalt
Metatexite
Diatexite
Partial melting

ABSTRACT

The conversion of basaltic crust into a thick, buoyant felsic crust of tonalite-trondhjemite-granodiorite (TTG) composition has been a fundamental process in the Earth's evolution during the Archaean Eon (4.03–2.50 Ga). The proposition that TTGs have formed as a result of the partial melting of hydrated mafic rocks is now well corroborated by geochemical modelling and experimental methods although these processes have only rarely been tested or documented by field studies. Here, we investigate the migmatite structures and major and trace element geochemistry of the 2.9–2.6 Ga Lake Inari TTG-metabasalt terrain in northern Finland, in the Lapland-Kola Province of Arctic Fennoscandia. The Lake Inari metabasalts geochemically resemble the flood basalts of the Phanerozoic oceanic plateaus. The TTGs show overall high Si and Na/K characteristics and have two coeval and intermingled geochemical endmembers, the low-HREE and high-HREE TTGs. Their variable geochemical signatures may reflect internal magmatic processes such as mingling of magmas that have experienced different evolutionary paths in terms of source mineralogy, degree of partial melting, differentiation and migration. The bimodal TTG-metabasalt association shows various migmatite structures such as metatexites, metatexite-diatexite transitions and massive diatexites that have formed in response to the weakening of the crust, melt segregation, extraction, migration and redistribution (SEMR) processes, and synanatectic strain. Rafts of the metabasalts probably represent the remnants of a basaltic upper 'lid' layer. We interpret the Lake Inari terrain to represent a widespread migmatization in deeper layers of an overthickened basaltic plateau persisting above a mantle plume, consistent with a stagnant or sluggish lid tectonic setting. Our results suggest that the formation of buoyant TTGs by partial melting of plateau basalts might have set off the evolution of continents.

1. Introduction

The study of the Archaean (4.03–2.50 Ga) Earth is an increasingly lively research field and significant for understanding why the Earth became habitable. Central topics to this research are the nature and timing of the formation and stabilization processes of the earliest continental crust. Over the course of the Earth's 4.56 billion years of evolution, low-density felsic crust has separated from high-density material such as the ultramafic mantle and mafic crust and accumulated into large, buoyant landmasses, which, according to Chowdhury et al. (2021), first rose above the sea level due to isostatic compensation between 3.3 and 3.2 billion years ago. There is now a consensus within the research community that continental crust has formed by plate tectonic processes at least since the Paleoproterozoic Era, but how the early continents of the Archaean Earth were formed is still the subject of diligent research and intense debate.

There are several generally accepted constraints for the formation of the Earth's early continental crust. Most Archaean crust consists of high Si and Na/K tonalite-trondhjemite-granodiorites (TTGs). They have two geochemical endmembers with high-HREE and low-HREE signatures, the meaning of which is not yet fully understood. Geochemically identical TTGs have formed from Eoarchaean to Neoarchaean (Halla, 2018 and references therein) making up most of the Archaean crust preserved to this day. The results of both experimental and petrological modelling (Palin et al., 2016 and references therein) support the proposition that TTGs are the products of the partial melting of hydrated basalts.

* Corresponding author.
E-mail address: jaana.halla@helsinki.fi (J. Halla).

https://doi.org/10.1016/j.precamres.2024.107407
Received 4 April 2024; Received in revised form 21 April 2024; Accepted 22 April 2024
Available online 9 May 2024

However, despite half a century of TTG research, the research community has yet to agree on their geodynamic environments. In recent years, the opinions on the tectonics behind the origin of continents have strengthened in support of transition from a stagnant-lid through the sluggish-lid to active-lid tectonics, although it has been acknowledged that different processes may have acted at the same time in different places and the timing of the transition is still under discussion. Many studies support stagnant-lid tectonics and plume origin for TTGs (e.g., Bédard, 2018; Wyman, 2018; Johnson et al., 2019; Wu and Zhao, 2022; Joshi et al., 2022; Tarduno et al., 2023; Vandenburg et al., 2023) but opposing opinions have also been expressed, in support of an early onset of subduction at convergent plate boundaries (e.g., Garde et al., 2020; Kusky et al., 2021; Arndt, 2023; Nutman et al., 2024).

The number of studies on the TTGs around the world is rapidly increasing, but there are still gaps in our knowledge. Firstly, many TTG formations, sometimes called broadly 'grey gneisses' or 'banded gneisses', contain abundant amphibolite rafts of different sizes and shapes giving them a 'black and grey' appearance. Although the formation of TTGs as the result of the partial melting of hydrated mafic rocks is well established in the literature (Moyen and Martin, 2012), less

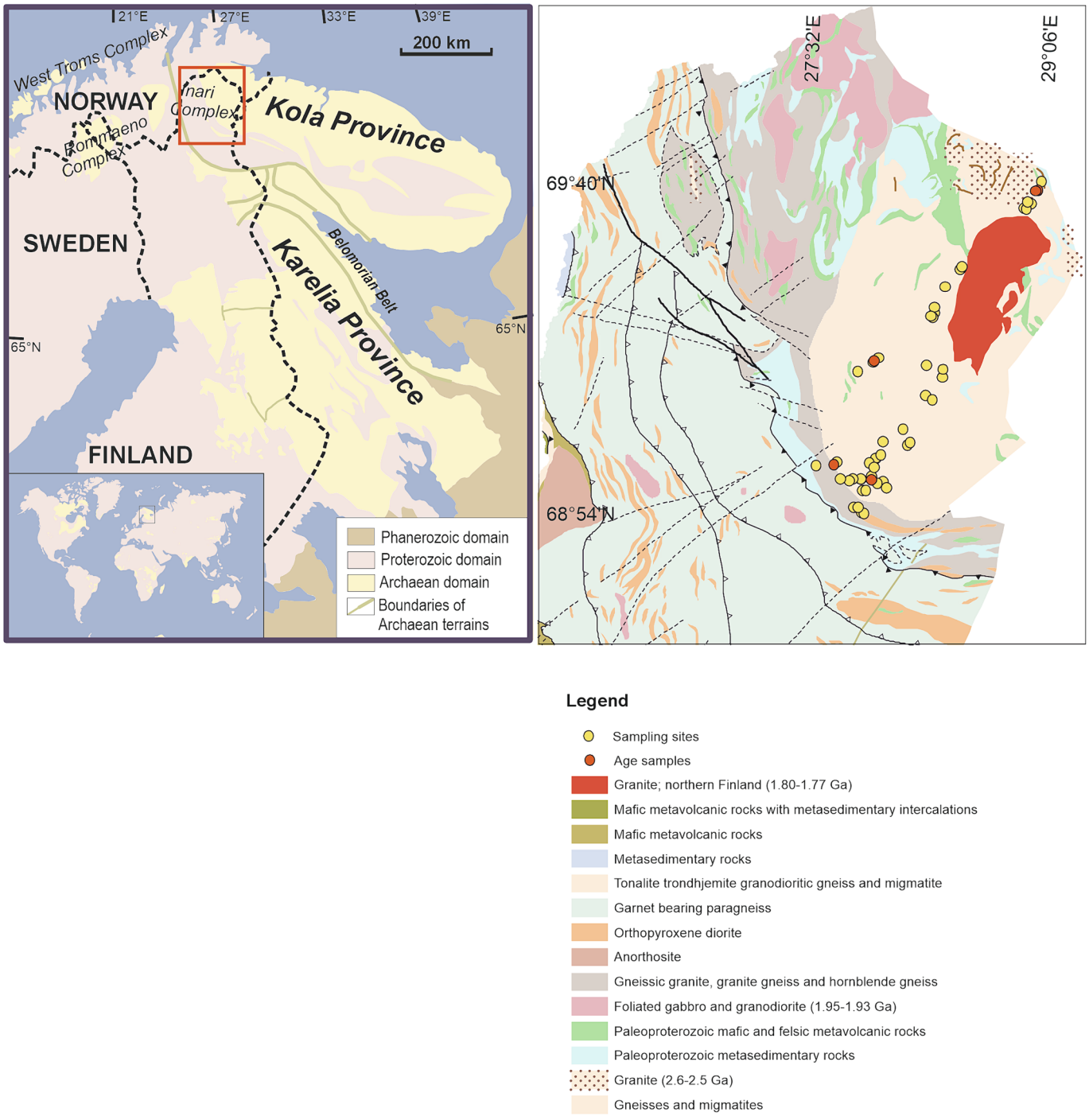

Fig. 1. (Left) Simplified map showing the Archaean complexes above the Arctic Circle: Lake Inari complex/terrain of the Lapland-Kola Province (2.9–2.6 Ga), Rommaeno Complex of the Norrbotten Province (3.2–2.7 Ga) and West Troms Basement Complex (3.0–2.8 Ga). The Archaean rocks of the Lapland-Kola Province are separated from those of the Karelia Province in the south by the Belomorian Mobile Belt. **(Right)** Sample locations (circles) shown on the geological map of northern Finland. The geochronological data for samples marked with red circles is available in Joshi et al. (2024).

attention has been paid to the amphibolites, which might represent the remnants of the basaltic source of the TTGs. This is one of the main themes of this paper, because the lack of knowledge of the relationships between TTGs and amphibolites and the scarceness of structural studies hinders our understanding of the processes involved.

Secondly, since the work of Barker and Arth (1976) dividing TTGs into the low-Al and high-Al types, research has demonstrated that TTGs form a geochemically heterogeneous group of igneous felsic rocks (Moyen and Martin, 2012 and references therein). HREE-enriched (Halla, 2009; Moyen, 2011) and K-enriched (e.g., Rollinson, 2021; Joshi et al., 2017) groups have been recognised, alongside the 'classical' TTGs characterised especially by low HREE contents. Although some studies have documented TTG terrains in which both the low-HREE and high-HREE types are closely associated (Mitra et al., 2017; Halla, 2018), these studies have not focused much on their spatial and temporal relationships. Hence, in this study, we pay special attention to the relationships between TTGs and amphibolites as well as between the high- and low-HREE TTGs. We will show that the Lake Inari amphibolites are metamorphosed basalts and, to avoid confusion, we use the term metabasalt hereafter.

This study contributes to the research on the origin of early continents by finding answers to the following research questions: 1) What is the nature and origin of the metabasalt rafts, and could they represent feasible source material of the TTGs? 2) What are the distribution and possible sources of the high- and low-HREE TTGs? 3) What are the rheological constraints on the TTG formation by migmatization? 4) What was the tectonic setting in which the bimodal TTG-metabasalt terrain formed?

To answer these research questions, we have studied well-exposed outcrops of TTGs and metabasalts north of the Arctic Circle in northern Fennoscandia, on the shores and islands of Lake Inari as well as along the Kaamanen–Näätämö road (Route number 971) to the northern side of the lake. The Lake Inari terrain (Fig. 1) consists of folded and banded TTG gneisses with abundant metabasalt rafts showing variable migmatite structures (Halla, 2020), thus providing an outstanding natural laboratory for studying TTG formation. Previous studies (Meriläinen, 1976) had identified the Lake Inari terrain as an Archaean granite-gneiss complex and Huhma (2019) provided a comprehensive report on the geochronological data that have been acquired in the past. Although the Archaean ages are well constrained, no modern geochemical studies have been carried out in the area. The original Archaean tectonic setting of the terrain is unknown, but its role in the Paleoproterozoic Lapland-Kola orogeny as a part of a colliding and overthrusting piece of Archaean crust has been explained by Lahtinen and Huhma (2019). The terrain formed by long-term migmatization between 2.9 and 2.6 b.y.a (Joshi et al., 2024).

Based on structural, geochemical and geochronological constraints, we argue that prolonged partial melting of a basaltic plateau may have formed the bimodal TTG-metabasalt association. After giving an overview of the current ideas of TTG research, we provide evidence for this argument by studying the structures and geochemistry of TTGs and metabasalts of the Lake Inari terrain. We interpret the results in the light of geochronological constraints presented by Joshi et al. (2024). Finally, we discuss the origin of the Lake Inari terrain with a focus on the structural relationships of the TTGs and metabasalts in the view of crustal rheology and the mode of occurrence of the high- and low-HREE TTGs. Our results and conclusions summarised in the final section provide insights into the formation of Archaean TTG-metabasalt terrains.

2. TTGs and tectonics

The acronym TTG for gneisses of tonalite-trondhjemite-granodiorite composition was first coined by Jahn et al. (1981). Today we know that TTGs form most of the Earth's Archaean crust. The study of TTG terrains started at the turn of the 1960s and 1970s with petrographic and geochemical studies and continued along with the development of geochronological and isotope methods, revealing the sodic nature, Archaean ages and mafic sources of TTGs. Moyen and Martin (2012) presented a thorough review of the development of the TTG concept, thus we will not recapitulate the full history here, we are focusing on the most recent studies.

TTGs commonly show complex metamorphic, deformation and folding structures in the field. Halla (2020) demonstrated the migmatitic nature of the banded TTG gneisses, suggesting that instead of treating them as granitoid plutons in the strict sense, they should be considered as a mass of flowing diatexites (high-degree partial melts) that do not form plutons *sensu stricto*. The diatexites enclose basaltic rafts (metatexites) in different sizes, shapes and partial melting stages. Contrary to the traditional concept of plutons, TTGs can be regarded as flowing crystal mushes (Weinberg et al., 2021) mingling with each other and/or assimilating country rocks. The metabasalt rafts probably represent remnants of a basaltic crustal 'lid' broken up by the partial melts. However, some TTG melts may well have separated from their migmatite sources and accumulated to form plutons above the present denudation level.

TTGs have two geochemical endmembers in the spectrum of REE patterns, called the low-HREE and high-HREE TTGs (Halla et al., 2009) that correspond to the high-pressure and low-pressure TTGs of Moyen (2011) and with the high-Al and low-Al TTGs of Barker and Arth (1976). The low-HREE TTGs show high SiO_2 and low MgO contents and elevated La/Yb, Sr/Y and Nb/Ta ratios, whereas high-HREE TTGs show a slightly larger range of SiO_2 and higher MgO contents and lower La/Yb, Sr/Y and Nb/Ta ratios.

The concept of high-, medium- and low-pressure TTGs of Moyen (2011) poses the requirement of partial melting in the deep crust, which has been argued to be difficult to trigger (Arndt, 2023). However, today there seems to be a consensus among researchers that the geochemical differences in TTGs are not direct reflectors of the pressure, i.e., depth of melting, but rather a consequence of fractional crystallisation of hornblende and plagioclase at relatively low pressures (Laurent et al., 2020; Liou and Guo, 2019; Rollinson, 2021; Kendrick et al., 2021; Mathieu, 2022; Smit et al., 2024). If true, this finding would reduce the requirement for deep melting and allow TTG formation at shallower crustal levels, such as overthickened basaltic plateaus.

According to the studies of Kendrick and Yakymchuk (2020), the geochemical signatures of TTGs may be garnet-controlled as well. They claimed that garnet fractionation is possible at lower temperatures than previously thought. Their modelling results imply that TTG trace elements are sensitive to fractionation into peritectic garnet during migmatization. Furthermore, TTGs could have inherited the low HREE signature from a fractionated source. According to Hole at al. (2023), fractional crystallisation of garnet in Paleogene plume-related alkali basalts caused increasing LREE enrichment and HREE depletion with decreasing whole-rock MgO, which is a trend shown by the steep REE patterns of low-HREE TTGs. Pourteau et al. (2020) reported similar geochemical varieties in post-Archaean TTGs and suggested the availability of fluids rather than melting depth as the cause.

Since the studies of Rapp et al. (1995), it has been generally accepted that TTGs are formed by the partial melting of hydrated (Murphy et al., 2024) basalts, but Smit et al. (2024) suggested rutile- and garnet-bearing plagioclase-cumulates in the roots of the protocontinents as a viable source of TTGs. Regarding the tectonic setting, the debate has fluctuated between subduction vs. mantle plume origin for TTGs using evidence from their geochemical differences. Joshi et al. (2024) discovered that the geochemical endmembers of TTGs occur in too close spatial and temporal association to be regarded as representing different tectonic settings. Based on redistribution models of heat-producing elements during partial melting of Archaean crust (Kinney et al., 2023), enriched basalts are the most viable sources of TTG magmas, and the mantle is at least an equal source of heat for metabasalt anatexis than radiogenic heat production.

Stagnant-lid convection, where subduction and surface plate motion

are absent, is common among the rocky planets and moons in our solar system, and also suggested for the early Earth (Bédard, 2018). Tarduno et al. (2023) reported identical paleointensities for primary magnetite inclusions in 3.9–3.3 Ga detrital zircons from the Barberton Greenstone Belt in South Africa. These results support unvarying latitudes pointing to stagnant-lid tectonics. Based on spatiotemporal distribution of granitoid trace element geochemistry, Vandenburg et al. (2023) suggested that rift-assisted breakup of protocratons is a viable mechanism for Archaean craton growth, which does not require active-lid tectonics. Geochronology of the Lewisian gneisses (Taylor et al., 2019) and the Lake Inari terrain (Joshi et al., 2024) indicate prolonged magmatism pointing to long-term plume activity. Consequences of stagnant-lid tectonics could include upwelling of asthenosphere and mantle-derived mafic melts as plumes and subsequent lithospheric delamination triggered by gravitational instability (e.g., Liu et al., 2024). According to Pourteau et al. (2020), some post-Archaean occurrences of TTGs are associated with upper amphibolite-facies metamorphism of enriched tholeiitic basalt and they pointed out that anatexis of flood basalts appear to have been the only way of TTG production since the end of the Archaean.

Despite the recently increasing observations supporting stagnant-lid tectonics, several authors support the present-day style of convergent tectonics, finding evidence for Archaean subduction. Copley and Weller (2024) suggested that present-day style of plate tectonics prevailed already in the early Archaean, but a higher rate of radiogenic heating affected the crustal rheology and the embodiment of convergent tectonics. Nutman et al. (2024) provided evidence for an early convergent plate boundary from the Eoarchaean Isua mafic–ultramafic assemblages in Greenland. For the origin of the North Atlantic Craton of West Greenland, Garde et al. (2020) favoured horizontal interthrusting and folding in a mainly convergent tectonic regime. According to Kusky et al. (2021), dome-and-basin structures of the Paleo-Mesoarchaean Pilbara craton are similar to those present in collisional orogens of the Phanerozoic record.

3. The Lake Inari terrain

In the northern parts of the Fennoscandian Shield of the East European Craton, Mesoarchaean to Neoarchaean complexes and terrains (Fig. 1) outcrop sporadically from Norway through Sweden and Finland to the Kola Peninsula (e.g., Lahtinen and Huhma, 2019; Karinen et al., 2015; Laurent et al., 2019; Myhre et al., 2013). These consist of folded and banded TTG gneisses enclosing metabasalt rafts in various sizes and shapes. Since the complexes in northernmost Fennoscandia fall in different countries and different provinces (the Lapland-Kola, Norrbotten and West Troms provinces) and are located north of the Arctic Circle, we have collected them under the term Arctic Fennoscandian Archaean terrains. Here, we use the term terrain instead of terrane because the boundaries are not known.

The orogenic Lapland-Kola Province consists of the Paleoproterozoic Lapland Granulite Belt (LGB) and Archaean to Paleoproterozoic Inari Complex. Hereafter, the Archaean part of the Inari Complex is termed the Lake Inari terrain.

According to the proposed tectonic model for the Paleoproterozoic Lapland-Kola Orogeny (Lahtinen and Huhma, 2019 and references therein), two Archaean continents collided around 1.9 b.y.a. because of subduction directed from northeast to southwest. In the northeast, a foreland basin was formed in front of the mountain belt when the lower plate flexed downward in response to an added load of thickened crust. In the southwest, an arc (Inari Arc), was formed on the overriding Archaean continent. Behind the Inari Arc, a retroarc basin and foreland were formed. The basin filled with sediments and metamorphosed to become the LGB. During orogeny, the Archaean rocks (the Lake Inari terrain) overthrusted the overriding crust as an out-of-sequence thrust nappe in response to orogen-parallel shortening. Cooling of the Lapland-Kola orogen culminated in the intrusion of post-tectonic granites at 1.79–1.76 Ga (Heilimo et al., 2009, 2014).

Ca. 1.9 Ga lower temperature metamorphism associated with the Lapland-Kola orogeny, temporally associated with the formation of the LGB and Inari Arc, caused minor zircon recrystallisation in the Lake Inari terrain, but the tectonic event did not influence the morphology of the terrain or cause widespread reworking or isotopic resetting (Lahtinen and Huhma, 2019). The Lake Inari terrain has mainly retained its primary Archaean character.

The Lake Inari terrain in Finnish Lapland is located on the edge of the Kola Province. The lake, together with its 3318 islands, lies in a depression formed by block faulting during the Paleogene–Neogene uplift of northern Scandinavia (Riis, 1996). Boundaries between the blocks, faults and fracture zones are still visible in the present landscape as rectilinear or gently winding valleys and bays, straits and lake depressions (Kujansuu et al., 1998).

The Lake Inari consists of a bimodal TTG-metabasalt association, which is exposed on the islands of Lake Inari and on the northern side of the lake. The southernmost part of the lake belongs to the Paleoproterozoic LGB and the northern part to the Lake Inari terrain. TTGs are the most abundant rocks, but there are many small, flat islands consisting solely of metabasalt as well as abundant metabasalt rafts on the island shorelines. The FIRE seismic reflection line (Patison et al., 2006; Joshi et al., 2024) transects the terrain along the Näätämö-Kaamanen road on the northern side of the lake.

The TTGs of the Lake Inari terrain have been dated by the U–Pb zircon method to have formed between 2.9–2.6 Ga (Meriläinen, 1976; Huhma, 2019; Lahtinen and Huhma, 2019). They are cut locally by pegmatitic dykes and porphyritic granitoids on the northern side of the lake. According to Joshi et al. (2024), a large time spread in zircon populations suggests a prolonged magmatic activity in the TTG terrain from 2.9 to 2.6 Ga, supporting a rather protracted and stationary source of heat such as a stagnant mantle plume with restricted relative movement between the plume and the overlying lithosphere. Taylor et al. (2019) reported similar age results from the Lewisian Complex, northwest Scotland pointing out, with the help of trace element data in zircon, that a continuous spread through Neoarchaean is not due to Pb loss by diffusion but reflects a persistence of melt-bearing crust for hundreds of millions of years.

4. Migmatite structures

The Lake Inari terrain consists of migmatites generated by different degrees of partial melting of a mafic source (Halla, 2020). Here, we describe the migmatite structures according to the morphological divisions presented by Sawyer (2008). The first-order division is based on the melt fraction and the properties of solid grains. The two-fold first order morphology divides rocks into low-melt fraction metatexites and high melt-fraction diatexites. The second order morphological division combines the melt fraction with the synanatectic strain, the latter causing the redistribution of the former.

The migmatite morphology formed in different melt fraction and strain regimes reflects partial melt segregation, extraction, migration and redistribution (SEMR) processes. SEMR is our proposed acronym to describe the whole process of partial melting from the first tiny interstitial drop to the redistribution of massive flowing diatexites (Cruden and Weinberg, 2018). The structures of Lake Inari migmatites formed in different melt fractions and strain regimes are illustrated in Figs. 2 and 3.

4.1. *Very low/low melt fraction – Low-strain regime*

The metabasalts of the Lake Inari terrain show metatexite structures from films to folds (Fig. 2). At very low melt fractions, only a small amount of melt segregates at the interstices of mineral grains and the metabasalt protolith remains coherent. The first sign of the onset of *in situ* partial melting is the formation of quartz-feldspar films along grain boundaries as manifested by a ‘white sugary’ texture of some

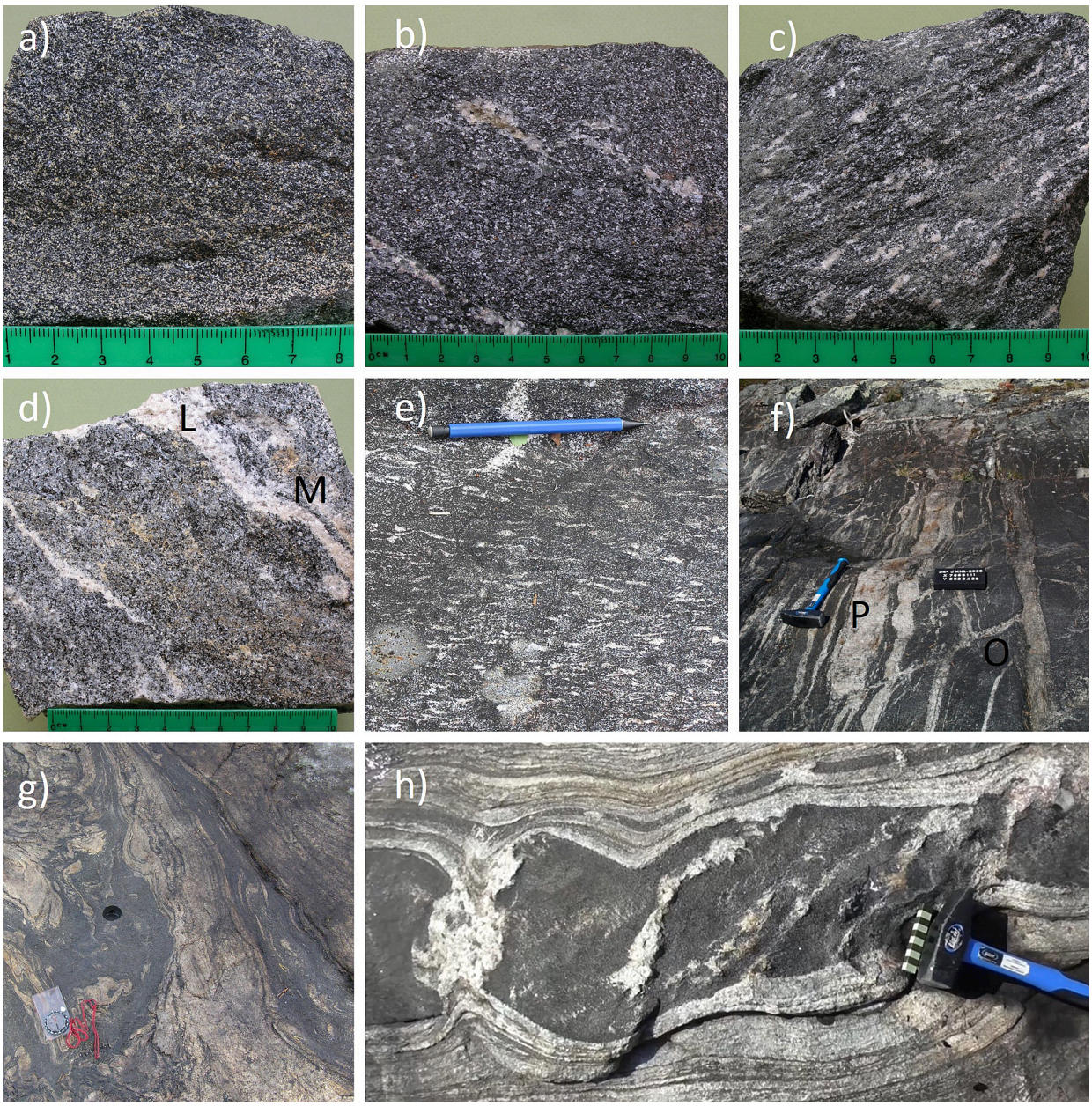

Fig. 2. Textures for melt extraction in a very low-melt fraction and low-strain regime (a–e) and metabasalt metatexite structures formed in a low-melt fraction and increasing strain regime (f–h). **(a)** The first small melt droplets crystallise into quartz-feldspar films along the grain boundaries. In this sample, they have turned white due to weathering, creating a sugary texture. Sample L1.2, film metatexite, Koutukinsaari Island. **(b)** Incipient partial melting has produced small, elongate patches of neosome. Sample L6.2, patch metatexite, Vieppisaaret Island. **(c)** This sample shows small mottles and strips of neosome. Sample L2.2, patch metatexite, Koutukinsaari Island. **(d)** Segregated in source leucosome vein (L) and a melanosome (M) in a metabasalt sample. With increasing melt fraction, veins may interconnect to form a network for melt migration. Outcrop L5, Palkissaari Island. **(e)** A metabasalt outcrop with a small proportion of neosome as films, patches, pockets, and veinlets. Outcrop L36, Tuurakivensaari. Outcrop L28, dilation metatexite, Kahkusaari Island. Length of scale 10 cm. **(f)** Stromatic (parallel-layered) structure showing incipient development into a net structure indicated by a set of leucosomes oblique (O) to the parallel layers (P) suggesting brittle conditions. Outcrop L34, stromatic (layered) metatexite, Kärppäsaari Island. **(g)** Different types of folds are formed as the melt fraction and strain increase. Outcrop L33, folded metatexite, Kärppäsaari Island. **(h)** In dilation structures, leucosomes are in low-pressure sites such as interboudin partitions, pressure shadows or fractures. This outcrop shows a boudin structure with coarse-grained leucosomes at low-pressure sites. Kärppäsaari Island. Photos Pekka Kivimäki

metabasalts (Fig. 2a). As the melt fraction increases, the films develop into patches or veinlets. In this regime, the melt has not separated from the rock that is still considered a metabasalt. Many samples of the Lake Inari metabasalts contain patches and veinlets that are often oriented along foliation planes (Fig. 2b–e). The metatexites may occur as large blocks of tens to hundreds of metres within the diatexites (Fig. 3a–b).

4.2. *Low melt fraction – Increasing-strain regime*

At low melt fractions, increasing synanatectic strain causes melt extraction into dilation (low-pressure) structures and veins. Parallel and laterally continuous leucosomes form a layered, stromatic structure, which, together with obliquely oriented leucosomes, define a net-like pattern of veins acting as channels for magma flow (Fig. 2f). Increasing melt fraction and strain produce folded metatexites with a wide range of leucosome orientations (Fig. 2g). In boudinage structures,

Fig. 3. Structures of the metatexite-diatexite transition zone (a–f) and massive diatexites (g–h). **(a)** A small flat island consisting solely of metabasalt. Outcrop L17, Hirvassaaret Islands. Metabasaltic islands can often be recognised from their low-lying relief. **(b)** Incipient break up of a large (tens of metres in diameter) block of metabasalt by migrated melts. Outcrop L25, metabasalt, Aikionniemi. **(c)** Rafts of metabasalt disaggregated by migrating diatexite melt. Outcrop L28, raft diatexite, Kahkusaari. **(d)** Rounded, rotated and dispersed rafts within the diatexite. Some of them show sharp edges. Outcrop L28, raft diatexite, Kahkusaari. **(e)** Diatexite flow bands wrapping around a metabasalt raft. The sharp, highly oblique contact excludes the alternative of a syn- or postmagmatic mafic intrusion. The structure is enhanced by weathering on the shore of Lake Inari. Outcrop L13, raft diatexite, Suovasaari. **(f)** Deformation and folding separate and stretch rafts into bands and schlieren. A boulder of folded raft diatexite, Näätämö. **(g)** Massive diatexite. Sample from Outcrop R3, low-HREE tonalite, Aitajärvet. (**h**) Massive diatexite. Sample from Outcrop R8, high-HREE tonalite, Jääjärvi. Length of scale in c), d) and f) 50 cm, in e) 20 cm, and in g) and h) 10 cm. Photos Pekka Kivimäki.

coarse-grained leucosomes occupy the low-pressure sites such as interboudin partitions, pressure shadows or fractures (Fig. 2h). In this regime, the magma migrates a shorter distance than in the next regime.

4.3. *Increasing melt fraction and high-strain regime*

In the increasing melt fraction and high strain regime (Fig. 3), the metabasalt completely loses its coherency and the melts start to migrate. Competent layers are progressively disrupted into tabular fragments of palaeosome (not melted part of the rock) or residuum (the solid fraction left after partial melting) that form rafts in diatexite. The metatexite-diatexite transition structures are common in the Lake Inari terrain, but they are especially well exposed in the increasing melt fraction and strain regime of the Kahkusaari Island, where voluminous migrating melts started to break up the metabasalt as indicated by a distinct sequence of metatexite-diatexite transition structures (Fig. 3b–d, Supplementary video). First, a metatexite layer breaks up into large rafts, which further disaggregate into smaller rafts. Due to shear stresses, magma flows easily, and flow bands are forming around the rafts (Fig. 3e). Because of increasing strain, a flowing diatexite melt tears off schlieren (streaks or swirls) from the rafts. A banded structure may form when the rafts strain and fold to form layers parallel to the flow-banding (Fig. 3f).

4.4. High melt fraction and high-strain regime

At high melt fractions and strain, the metabasalt completely loses its cohesion, which leads to the formation of a massive diatexite. Diatexite melts may rise upwards due to buoyancy, flow laterally in the mid crust, or separate and emplace as TTG plutons *sensu stricto*. Massive diatexites are common along the Kaamanen–Näätämö road on the northern side of Lake Inari (Fig. 3g–h). Large volumes of flow-banded diatexite manifest the most advanced stage of migmatization. They show schlieren structures and occasional vestiges or ghosts of metatexites partially or almost completely digested by the diatexite. The vestiges may have an aureole of a weakly oriented, coarse-grained leucosome indicating partial melting of metatexites within the diatexites. In other words, massive diatexites are a complex mixture of both local and migrated melts. Massive diatexites are more common along the Näätämö road than on the islands of Lake Inari, which show more transitional metatexite-diatexite structures.

5. Geochemistry

We have sampled 52 outcrops of the Lake Inari terrain from lake shores and islands and along the Kaamanen–Näätämö road for the geochemical analyses. The sample set of 90 samples consists of TTGs and associated metabasalts, mostly collected from next to each other as pairs, showing various migmatite structures as described in Section 4. Figs. 4–8 illustrate the results. The Supplementary material gives the major and trace element data and coordinates (S1), additional plots (S2), photos of the samples (S3), and a video on the Kahkusaari outcrop L28 (S4).

5.1. Metabasalts

The metabasalt rafts described in section 4 consist of plagioclase and hornblende, minor quartz and K-feldspar, occasional pyroxene and, very rarely, garnet. The leucosomes of the metatexites contain plagioclase, quartz, hornblende and biotite. Geochemically, most of our amphibolite samples can be classified as basalts based on the TAS diagram (Fig. 4). Generalising, we consider that our whole-rock data correspond to the composition of mafic protoliths, i.e., incipient partial melts have been immobile on sample scale. Nevertheless, we associate the alkaline affinity and unusually high Na_2O contents in three samples with mobility of sodium, possibly due to melt migration or alteration, as these samples have a low Nb/Y value typical of subalkaline rocks (Pearce, 2008). One sample has relatively high SiO_2 and plots in the field of basaltic andesite.

The amphibolite samples have variable MgO contents of ~ 10 to 3 wt % (Fig. 5) and Mg-numbers [molar Mg/(Mg + Fe^{2+}) assuming $Fe^{2+}/Fe_{tot} = 0.8998$] of ~ 65 to 23, but most of them can be described as low-Mg basalts. One ultramafic sample has a notably high MgO content (Fig. 5), and we describe this sample separately.

In the Mg-number vs. oxide plots (Supplementary material S2), the low-Mg samples define geochemical trends that are characteristic of tholeiites, i.e., decreasing Mg-numbers are coupled with enrichment of Fe_2O_3tot, TiO_2 and P_2O_5, and depletion of Al_2O_3 and CaO. The variations in Na_2O and K_2O show considerable scatter indicative of the mobility of these components during metamorphism or earlier alteration. Using the Ti/Y cut-off classification Scheme (Xu et al., 2001; Zhang et al., 2023), all the samples have Ti/Y < 500 making them low-Ti type. The peridotite-incompatible trace elements (e.g., Nb, Zr, Hf and Y) show a marked increase in concentrations along with decreasing Mg-numbers, with enrichment factors up to > 8 for Nb, whereas the contents of highly compatible elements decrease from relatively high to low values (Ni 160 to 40 ppm and Cr 350 to 30 ppm).

We have divided the low-Mg metabasalts into three groups based on their REE characteristics (Fig. 6a, normalising values from Sun and McDonough, 1989). Group 1 exhibits mild enrichment of light REE, with chondrite-normalised $(La/Yb)_N$ of 1–1.5. Group 2 is more enriched in light REE and has $(La/Yb)_N$ of > 1.5, and Group 3 is relatively depleted in light REE with $(La/Yb)_N < 1$.

The primitive mantle-normalised incompatible element patterns (Fig. 6b) of the metabasalt samples belonging to Group 1 and Group 2 are relatively uniform and flat. Many samples in Group 1 and Group 2 show mild enrichment of Ba and U relative to Nb, and Pb relative to Ce, however. The samples that exhibit the lowest contents of incompatible elements typically exhibit depletion in Nb and enrichment in Pb relative

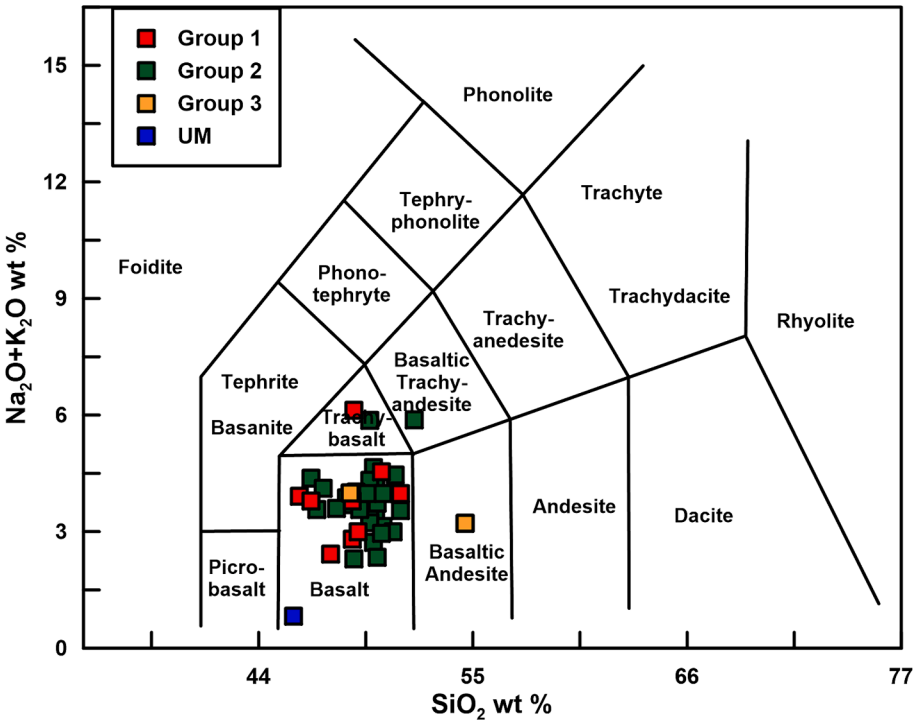

Fig. 4. TAS classification diagram for basalts. See Fig. 6 for the groups. UM = ultramafic.

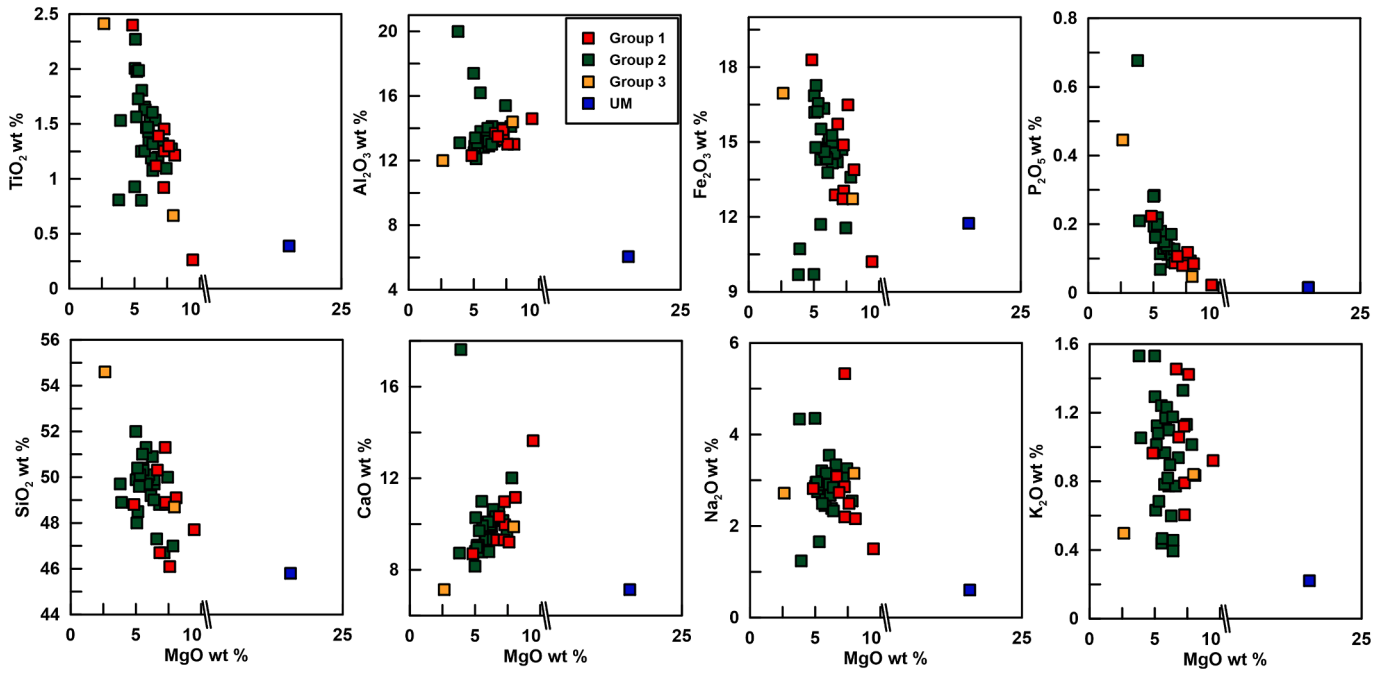

Fig. 5. Bivariate major and trace element vs. MgO plots for basalts. See Fig. 6 for the groups. UM = ultramafic.

to similarly peridotite-incompatible La and Ce.

In the case of our high-Mg ultramafic sample L06.1 Vieppisaaret, the contents of most major and minor oxides and peridotite-incompatible elements are low, whereas the Cr (~2500 ppm) and Ni (1400 ppm) contents are notably high. In the chondrite-normalised REE diagram, the ultramafic sample is distinguished by its strong relative depletion in light REE as well as its low REE contents in general and the mantle-normalised incompatible element pattern shows pronounced positive Ba, U and Pb anomalies.

5.2. TTGs

The TTGs consist mainly of plagioclase, quartz, minor K-feldspar, hornblende and biotite. Based on the data, all of them show high SiO_2, high Na_2O and low K_2O characteristics, but they fall in two groups based on some other elements. The first group has low-HREE contents, low Mg, higher Sr, lower Yb_N and higher Nb/Ta. The second group has high-HREE contents, a larger range of MgO contents, higher Cr and Ni contents, lower Sr, higher Yb_N and lower Nb/Ta (Supplementary material S1).

Fig. 7 shows classification and discrimination diagrams for TTGs that are described in Section 4. The diatexites are mainly tonalites, but also some granodioritic and dioritic varieties occur as shown in the PQ classification diagram (Fig. 7a) of Debon and Le Fort (1983). In the ternary classification (Fig. 7b) and source discrimination (Fig. 7c) diagrams of Laurent et al. (2014), tonalites plot mainly in the fields of TTGs and a low-K mafic source, respectively. Plots in the total $(HREE)_N$ vs. SiO_2 diagrams (Fig. 7d) and $(Gd/Er)_N$ vs. MgO plot (Fig. 7e) clearly illustrate the difference in the HREE and MgO contents between the low- and high-HREE TTGs. We will further discuss the differences between the high- and low-HREE TTGs in Section 6.2 (Fig. 10). Based on the REE patterns (Fig. 8a), the TTGs divide into 3 main groups: 1) high-HREE TTGs, 2) low-HREE TTGs with positive Eu anomaly and 3) low-HREE TTGs with negative Eu anomaly. Fig. 8b plots the spider diagrams for TTGs.

6. Discussion

Researchers generally agree that Archaean TTGs were formed by the partial melting of hydrous basalts although the geodynamic setting in which this occurred remains debated (e.g., Wu and Zhao, 2022). Here, we add a new perspective to the discussion by providing an interpretation of the migmatite structures and geochemical features of an outstanding natural laboratory, the well-exposed Lake Inari TTG-metabasalt terrain in Arctic Fennoscandia. Together with the recent geochronological study of Joshi et al. (2024), our results enlighten the research questions on 1) the origin of metabasalts and their feasibility as the sources of the TTGs, 2) the distribution and sources of high- and low-HREE TTGs, 3) rheological constraints for the migmatization of the metabasalts and 4) insights into the tectonic setting of the formation of the TTG-metabasalt terrain.

6.1. Metabasalts

Archaean TTG terrains contain abundant amphibolites in various sizes and shapes as rafts, layers, bands, streaks and swirling folds. In the Lake Inari terrain, they represent basalts first metamorphosed in the amphibolite facies conditions and, thereafter, partially melted into variable metatexite forms (film, patch, vein, dilation and layered metatexites), sometimes folded or even digested by migrating diatexite melts. There has been ongoing debate whether the sources of basalts are related to subduction (e.g., Arndt, 2023) or plume environments (e.g., Wu and Zhao, 2022). Studies attempting to solve the problem by geochemistry and modelling (e.g., Huang et al., 2020) are more common than the structural studies of the TTG formations (Halla, 2020), so in that sense, we provide new insights to the discussion.

Based on our geochemical investigations (Section 5.1), the Lake Inari amphibolites are metabasalts (Fig. 4) that were formed from mantle sources (Fig. 9b–d). When addressing the geodynamic environment of mantle-source magmatism using metabasalt samples, it is critically important to constrain the possible geochemical influence of alteration and metamorphism. The immobility of high-field strength elements (HFSE) and REE during subsolidus processes is well known. We examined the correlations of the potentially mobile alkali and earth alkali metals U and Pb with the fluid-immobile Nb. The values of Rb/Nb (0.9–74), Ba/Nb (6–233), K/Nb (309–17000), U/Nb (0.02–0.6) and Pb/Nb (0.13–15) are almost invariably much higher than in the primordial mantle (PM) of McDonough and Sun (1995). This suggests a systematic

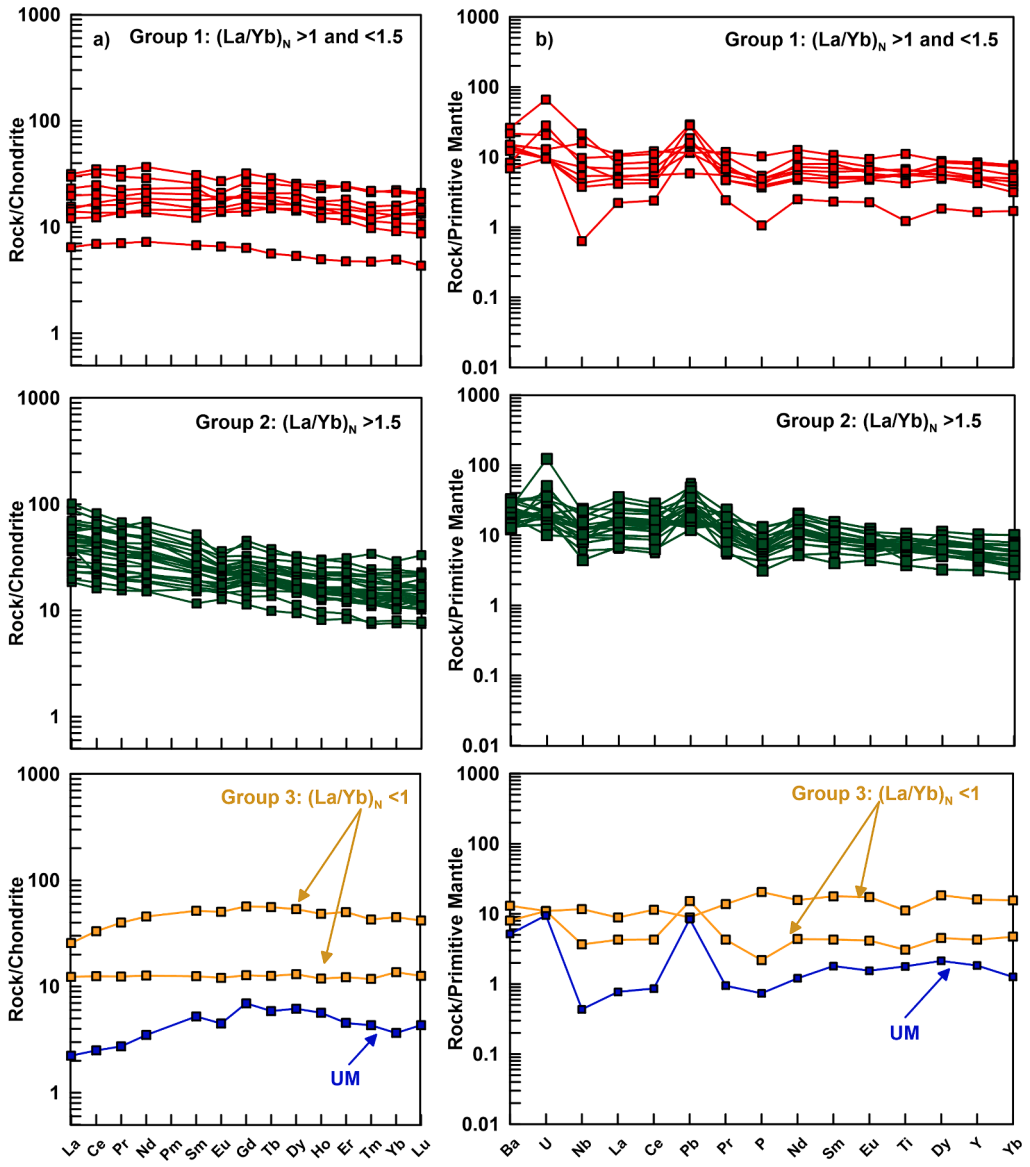

Fig. 6. REE-patterns **(a)** and spidergrams **(b)** for basalts. Normalisation values from Sun and McDonough (1989). UM = ultramafic.

enrichment in the fluid-mobile elements in the mantle source or during magmatic evolution, alteration or metamorphism.

The overall geochemical range of the metabasalt samples (Fig. 5) can be ascribed to fractional crystallisation. The increase in Fe_2O_3tot, peridotite-incompatible TiO_2 and P_2O_5, and most trace elements as well as the decrease in Al_2O_3, CaO, Cr and Ni when Mg-number decreases (Fig. 5) are the characteristic features of olivine and plagioclase fractionation from mafic magmas. Frequently, the possible assimilation of continental crustal wall rocks has been estimated by using contamination-sensitive indexes, such as Th/Nb, La/Nb and Pb/Ce (Thompson et al., 2001; Jackson et al., 2007; Xia, 2014; Zhou et al., 2020). In the case of the Lake Inari metabasalts, most of the samples show higher Th/Nb, La/Nb and Pb/Ce than PM and positive correlation between La/Nb and Th/Nb, which is consistent with variable contamination with wall rocks. The plots are not shown except for the Pb/Ce ratios against MgO in Fig. 9a. From the viewpoint of our preferred oceanic setting (below), we recognise the partial melting of mafic wall rocks as a possible source of contaminants. Bearing in mind the ample evidence of anatectic melting, we maintain that the observed variability in Th/Nb, La/Nb and Pb/Ce could equally well result from the migration of incipient melts during metamorphism.

For interpretations on the mantle source, we selected Samples L01.2 Koutukinsaari (Fig. 2a), L39.3 Varttasaari and R01.2 Sevettijärvi (Supplemetary material S3) that show the lowest and most PM-like ratios of contamination-sensitive Th/Nb, La/Nb and Pb/Ce. It should be noticed that these samples also record the lowest and most PM-like ratios of mobile elements and Nb, but we emphasise that our main conclusions are based on the characteristics of the immobile HFSE and REE.

Fig. 9(a–d) shows diagrams for basalts. Despite probable crustal contamination, most of our metabasalt samples lack marked Nb anomalies typical of basalts from volcanic arcs and their compositions fall mainly in the fields of mid-ocean ridge basalts (MORB) and oceanic island basalts (OIB) in the tectonic discrimination diagram Nb/La vs. La/Yb (Fig. 9c, Hollocher et al., 2012). The relative enrichment of Th causes most of the samples to plot outside the MORB-OIB array in the Th/Yb vs. Nb/Yb diagram (Fig. 9b, Pearce, 2008), however. Importantly, the samples that we regard to provide the most reliable geochemical data for uncontaminated magma compositions and mantle sources (L01.2 Koutukinsaari, L39.3 Varttasaari and R01.2 Sevettijärvi; indicated by sample numbers in Fig. 9(a, c–d) plot within the fields of MORB (and EMORB) and OIB in the diagrams of Pearce (2008) and Hollocher et al. (2012). Moreover, their PM-normalised incompatible element patterns

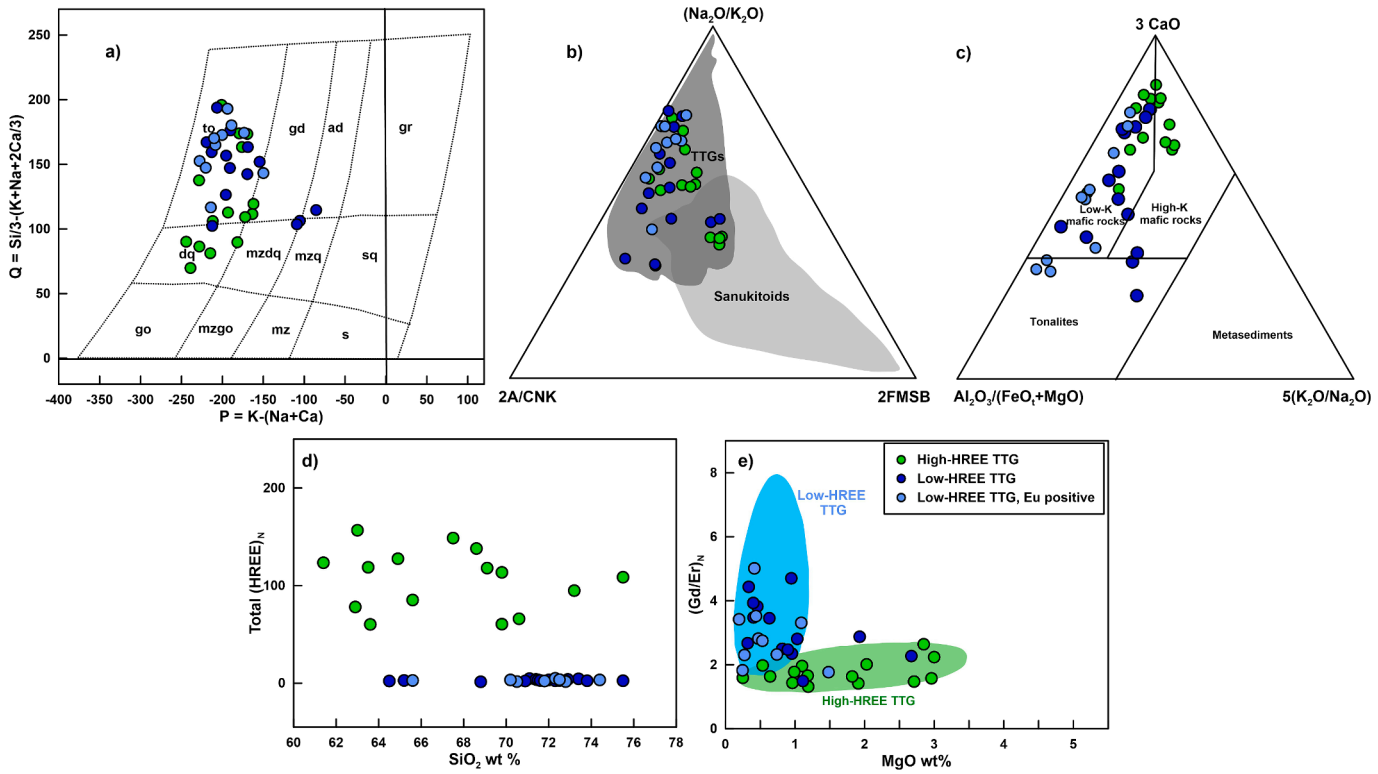

Fig. 7. Classification **(a–c)** and discrimination **(d–e)** diagrams for TTGs **(a)** PQ-diagram of Debon and Le Fort (1983). Ternary (b) classification diagram and (c) source discrimination diagram of Laurent et al. (2014). Tonalites plot mainly in the field of a low-K mafic source. **(d)** Total HREE vs. SiO_2, (e) $(Gd/Er)_N$ vs. MgO (Halla et al., 2009).
Source discrimination diagram of Laurent et al. (2014)

point to broad similarities to PM. In the modern tectonic settings, the compositions of samples L01.2 Koutukinsaari, L39.3 Varttasaari and R01.2 Sevettijärvi would be indistinguishable from enriched MORB and oceanic flood basalts, i.e., settings that are associated with hotspots. To illustrate this fact, we have compared our data with the Cretaceous oceanic basalts of the Ontong Java Plateau, which is the largest known igneous province preserved on Earth (e.g., Tejada et al., 2002; Chen et al., 2021), in Fig. 9d. We note in particular that the small negative anomalies at Sr and Ti in our low-Mg samples are likely to result from the fractionation of plagioclase and Fe-Ti oxides. It is also possible that the relatively higher Rb and Ba may record an addition of these mobile elements during hydrothermal alteration, if the mantle source was slightly depleted relative to PM as suggested by the mild depletion of Th, U and Nb relative to light REE in the PM-normalised patterns.

Overall, we conclude that compared with the Phanerozoic mantle-sourced magmatic rocks, the tholeiitic Lake Inari metabasalts are geochemically markedly different from most rocks in continental and subduction settings and, instead they resemble oceanic hotspot-related suites (e.g., Ontong Java). While the contents of several elements may have been affected by metamorphism and multiple alteration events, the relative abundances of most HFSE (e.g., Nb) and REE likely correspond to those of the mantle-derived parental magmas and allow the estimation of the mantle source compositions.

Discriminating the Archaean basalts is a difficult task because many of the criteria applied to fresh modern basalts cannot be directly adopted to possibly altered Archaean basalts, and the tectonic scenario might have been different from today because of the differences in the mantle temperature, thickness of the oceanic crust and depth of melting. Nevertheless, the mantle source of the Lake Inari metabasalts appears to have been a part of the convective mantle not affected by geochemical fractionation in subduction zone or MOR environments and, accordingly, we postulate the derivation of the mafic magmas from a mantle plume.

6.2. *Low-HREE and high-HREE TTGs*

The mode of occurrence of the different geochemical types of TTGs, i.e., their relationships, distribution and age, gives information on the tectonic setting in which they were formed. Coeval and intermingled TTG types of the Lake Inari terrain (Joshi et al., 2024) suggest an origin related to the internal magmatic processes and interplay of magmas experienced different paths of differentiation and migration. Based on the REE patterns (Fig. 8a), the Lake Inari TTGs divide into two main groups: low-HREE and high-HREE TTGs. The structural, geochemical and geochronological (Joshi et al., 2024) results show that both types of the Lake Inari TTGs represent the same age spread and can be found intermingled within the same area. Bivariate diagrams in Fig. 10 confirm that garnet-compatible elements Sc, Y, Zn and Co correlate positively with the HREE contents. Since the groups differ especially in their garnet-compatible elements, we interpret them as garnet-controlled although many authors consider plagioclase and amphibole fractionation as an adequate explanation for the differences in the TTG geochemistry (Laurent et al., 2020; Kendrick et al., 2021; Rollinson, 2021). The variation in the Eu anomaly of low-HREE TTGs from positive to negative may well reflect plagioclase accumulation/fractionation.

However, it is accepted that abundant TTGs of similar geochemical compositions were formed already in the Eoarchaean (e.g., Rollinson, 2023; Halla, 2018). The overall bimodality of TTGs remaining the same from Eoarchaean to Neoarchaean might be difficult to explain solely with the local fractionation of plagioclase and amphibole, and, perhaps, requires a more fundamental explanation for the differences persisting through time and space. Therefore, we would like to highlight some other points of view. Firstly, the Sc concentrations in garnets are seven times higher than the estimate for the silicate Earth, well above any

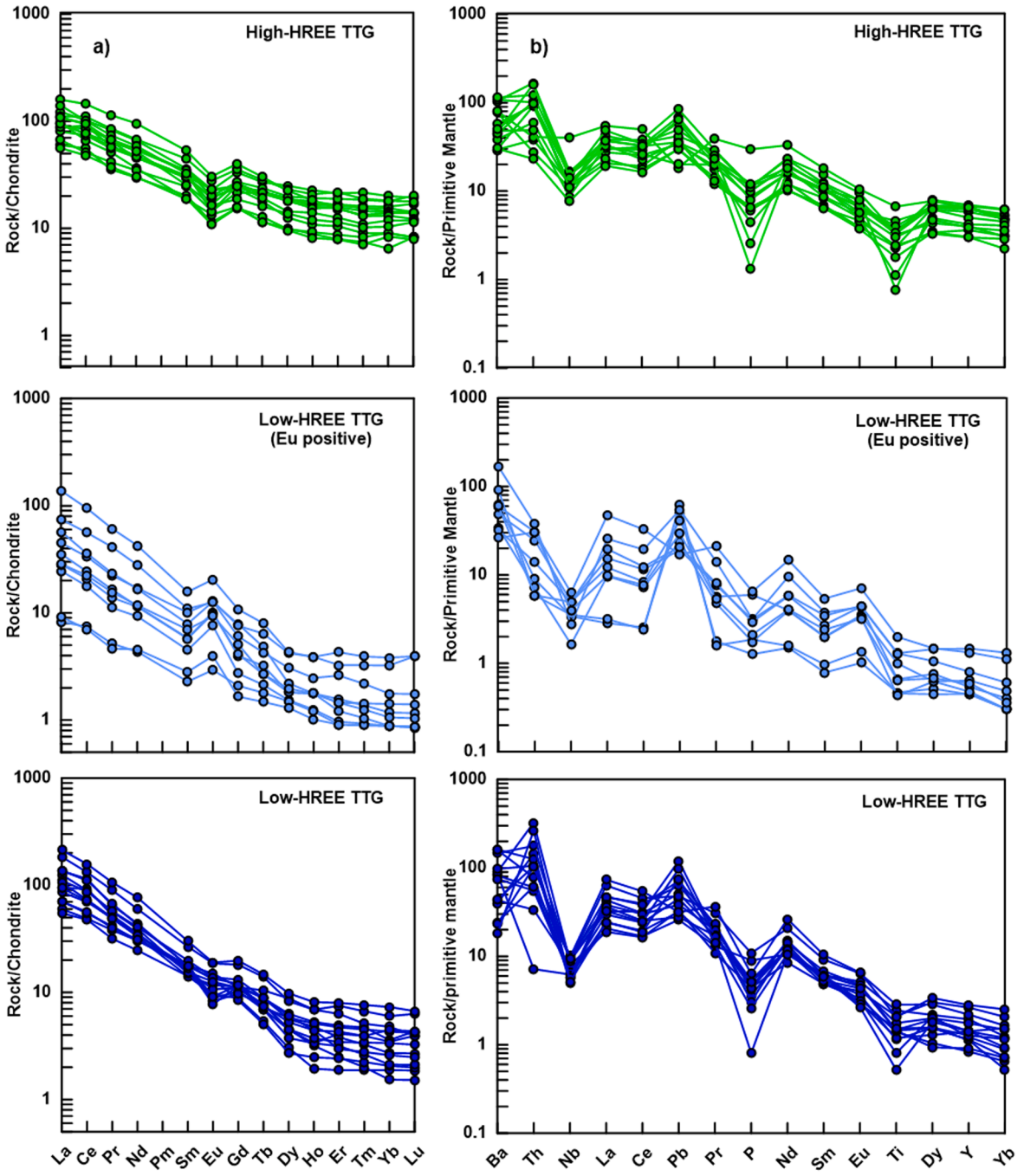

Fig. 8. REE patterns (a) and spidergrams (b) for TTGs. Normalisation values from Sun and McDonough (1989).

other mineral group (Chassé et al., 2018). Secondly, Hole et al. (2023) reported increasing LREE enrichment and HREE depletion and decreasing whole-rock MgO (a similar trend to what TTGs have) in Phanerozoic mantle-plume related alkali basalts due to the fractional crystallisation of garnet. Thirdly, the modelling results of Kendrick and Yakymchuk (2020) implied that the trace elements of TTGs are sensitive to fractionation into peritectic garnet during migmatization at lower temperatures than previously thought. Thus, we conclude that the garnet control cannot be ruled out and that the geochemical diversity of TTGs may be due to the fractionation of garnet, plagioclase and hornblende at different stages of the formation of the Lake Inari terrain. The fact that metabasalt rafts within the Lake Inari TTGs do not contain garnet (unless very rarely), but the low HREE-TTGs point to garnet fractionation, might reflect magma migration. Magma from a garnet-fractionated source may have induced melting in the amphibolite facies. This scenario would end up into a complicated mixture of low- and high-HREE crystal mushes. However, more research and data is needed to confirm these relations.

6.3. *Partial melting and rheology*

Migmatite structures are important indicators of partial melting processes and the rheology of the crust. Our structural investigations confirm that the Lake Inari bimodal TTG-metabasalt association shows variable migmatite structures that have formed in response to the increasing melt fraction and synanatectic strain, reflecting changes in the crustal rheology due to partial melting.

Previous theoretical, experimental and geological studies

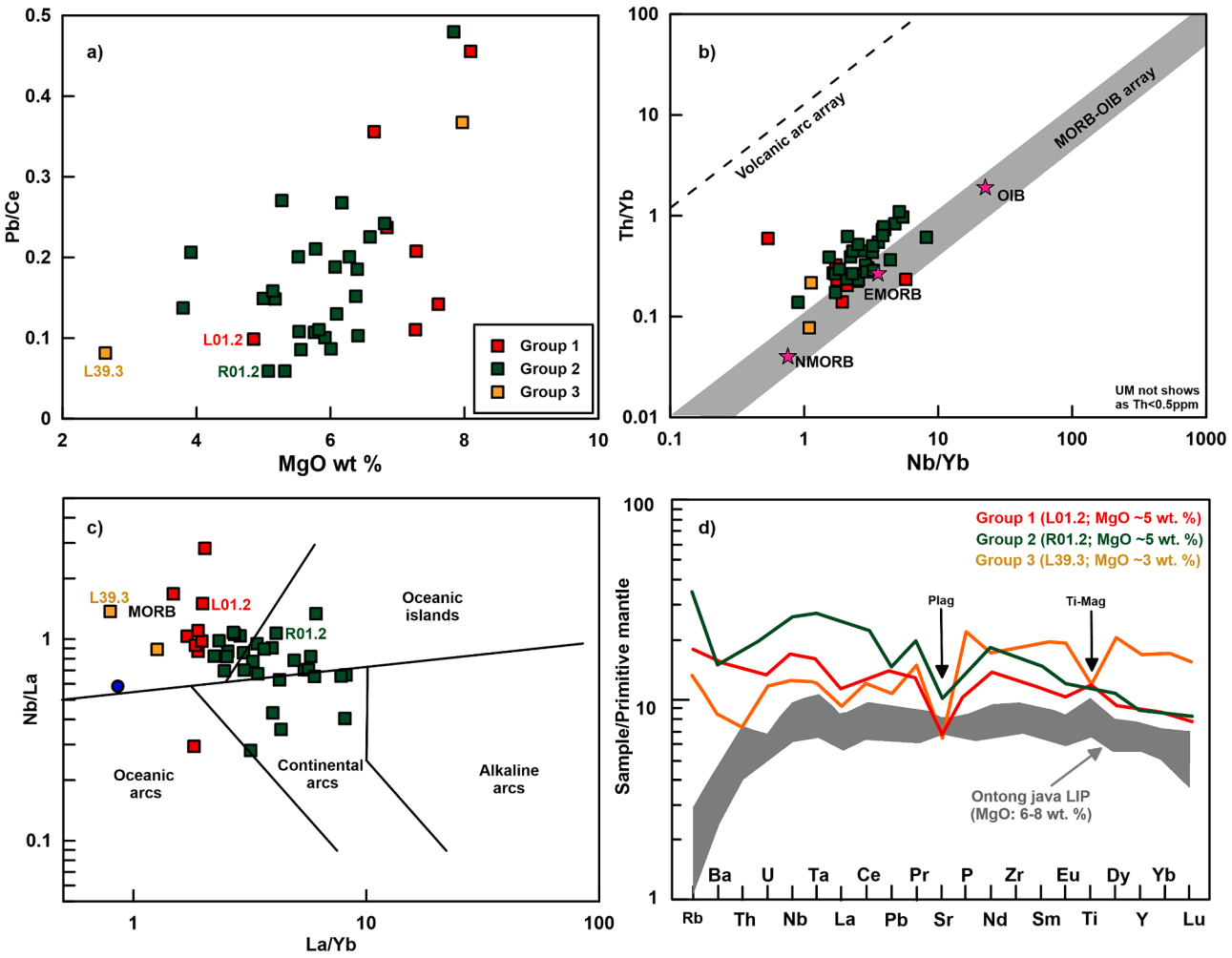

Fig. 9. Assimilation (a) and tectonic discrimination (b–d) diagrams for basalts. (a) Pb/Ce vs. MgO (b) Th/Yb vs. Nb/Yb (Pearce, 2008), (c) Nb/La vs. La/Yb (Hollocher et al., 2012), (d) Spider plot, comparison data of Ontong Java Plateau from Tejada et al. (2002). Normalisation values from McDonough and Sun (1995).

(Rosenberg and Handy, 2005; Chen et al., 2017; Zhang et al., 2019) elucidating the influence of the progressive partial melting of rocks on the rheology of the crust have revealed three rapid drops of crustal strength at certain melt fractions (7 %, 21 % and 41 %). Since the structure of a partially melted rock depends on its melt fraction, these drops of strength cause a sudden structural change. Therefore, to understand the origin of the Lake Inari migmatite terrain, we define the formation zones of the different migmatite structures. Based on the crustal strength drops, melt SEMR processes and synanatectic strain (Section 4), we identify five structural zones in the field. The zones are illustrated in Fig. 11 and explained below.

- *Protolith zone*. The first drop in the crustal strength at 7 % melt fraction is known as the Melt Connectivity Transition (MCT 7 %; Rosenberg and Handy, 2005). Below this transition, only small amounts of unconnected *in situ* melts may reside in the intergranular pore spaces of the rock. Structurally, they appear as film and patch metatexites (Fig. 2a–e). It seems that the least affected basalts within TTGs show flat REE patterns (Group 1 in Fig. 6), whereas basalts with small unconnected melt pockets show slightly enriched LREE patterns (Group 2 in Fig. 6). In this zone, the first tiny drops of melt start to segregate from the protolith at low strain conditions. The metabasalts of the Lake Inari terrain may represent an upper 'lid' layer broken up by migrating partial melts.
- *Metatexite zone A*. After passing the MCT 7 %, the intergranular melts in pore spaces start to extract, connect, and flow into thin foliation spaces of the rock. A framework of competent metabasalt layers with thin melt bands forms within the protolith. Narrow-banded metatexites continue forming from the MCT 7 % until the second drop of crustal strength occurs.
- *Metatexite zone B*. The second drop at a melt fraction of 21 %, the Framework Melt Transition (FMT 21 %; Chen et al., 2017) starts the transition from eutectic quartz-feldspar melting to refractory biotite melting. Increasing melt fraction and high strain produce layered and net-like structures providing effective channels for the magma flow (Fig. 2f) as well as folded metatexites with a wide range of leucosome orientations (Fig. 2g), Outcrop L33 Kärppäsaari). In this regime, the magma probably migrates only a very short distance within the rock showing typical 'in source leucosome' structures or travels longer distance away showing diatexite structures (Outcrop L34, Kärppäsaari). Metatexites are forming until the third critical drop in crustal strength occurs.
- *Metatexite-diatexite transition zone*. After the third drop at 41 % melt fraction, the Solid to Liquid Transition (SLT 41 %; Rosenberg and Handy, 2005), the metabasalt completely loses its coherency. Competent layers progressively disrupt into tabular fragments of protoliths, metatexites or residues that form diminishing rafts suspended in diatexites (Fig. 3a–f). In this zone, diatexite melts may flow from the diatexite zone, perhaps carrying an inherited low-HREE structure from the magma source (Outcrop L28 Kahkusaari).
- *Diatexite zone*. At very high melt fractions (possibly > 60, theoretical value from Sawyer, 2008) and strain, the metabasalt completely

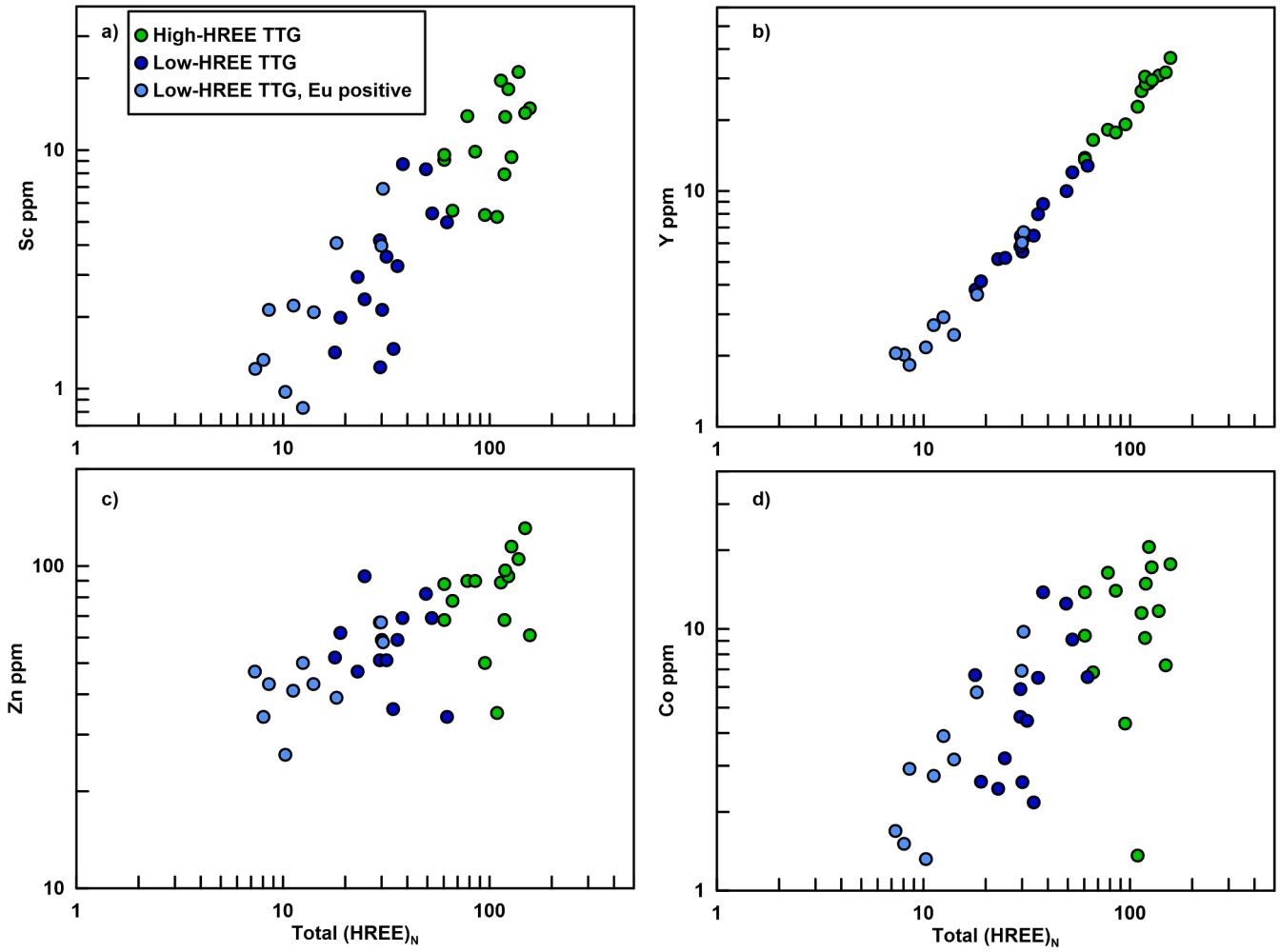

Fig. 10. Selected garnet-compatible elements Sc **(a)**, Y **(b)**, Co **(c)** and Zn **(d)** vs. total $(HREE)_N$.

loses its cohesion and massive diatexites are formed (Fig. 3g–h). The critical instability under a significant crustal loading might lead to rapid melt transfer to upper crustal levels. Diatexite melts may rise upwards due to buoyancy or flow laterally as a crystal mush.

The results of this study confirm that the migmatite structures of the Lake Inari terrain are controlled by the extent of partial melting and strain. Our field investigations indicate that the rocks visible on the present denudation surface were formed after passing the SLT 41 % in the metatexite-diatexite transition zone when the basaltic protolith lost its coherency and original structures. The competent layers of protolith, metatexite or residuum (the solid fraction left after the partial melting) were progressively disrupted into rafts and schlieren suspended and wrapped by flowing diatexite melts. Fig. 12 illustrates a flowing diatexite melt breaking up amphibolite into diminishing rafts with variable morphology as disaggregation proceeds. Accumulated metatexite melts produce leucocratic plagioclase-quartz pods. The photos are from the Singhbhum Craton India, but these structures are also common in the Lake Inari terrain.

The gneissic appearance of TTGs is due to the preferential orientation of minerals according to the magmatic flow (Fig. 3e). At high melt fractions, the basaltic protolith completely lost its cohesion and a massive diatexite TTG was formed. Diatexite melts have retained in the crust at the present denudation level, but in the upper, now denuded levels they may have separated and emplaced into TTG plutons. The loss of cohesion at high melt fractions coupled with buoyancy- and pressure-driven flow resulted in the abundance of diatexites over metatexites in the Lake Inari terrain. The large proportion of diatexites suggests that the lake Inari terrain was a buoyant, melt-rich crustal horizon retaining a substantial proportion of anatectic melt.

A 15 m high vertical profile of the Fuhuling metatexite-diatexite transition in South China shows an order of structures resembling the Lake Inari terrain, from top to bottom: parallel-oriented layered metatexites, variably folded metatexites, and raft and schlieren-structured diatexites (Zhang et al., 2019). However, vertical metatexite-diatexite profiles are not available in the Lake Inari region due to the low-relief landscape that lacks vertical surfaces such as cliffs and road cuts. The structures resembling the Fuhuling profile are observed only horizontally. Although it is uncertain what was the original stratigraphy of the zones, the results provide evidence of the origin of TTGs by the partial melting of a basaltic rock unit.

In terms of crustal architecture, the Lake Inari terrain represents a nappe overthrusted from northeast to southwest onto the overriding plate during the Paleoproterozoic Lapland-Kola orogeny (Lahtinen and Huhma, 2019). The metabasalts have a fine-grained texture and they lack garnets, which indicate that the terrain has not experienced high-grade metamorphism after its formation. Our samples represent a NE-SW oriented transection of the terrain from the boundary of the granulite belt to the country border (Fig. 1). The felsic flow-banded TTG crust shows metatexite-diatexite transitions that form an interconnected network in a rough scale of a few hundred meters. The sizes of metabasalt rafts vary from cm-scale to meter-scale and larger blocks are from tens to hundreds of metres in diameter. Furthermore, a few km-scale blocks are found in the Lake Inari terrain. Enveloping surfaces to

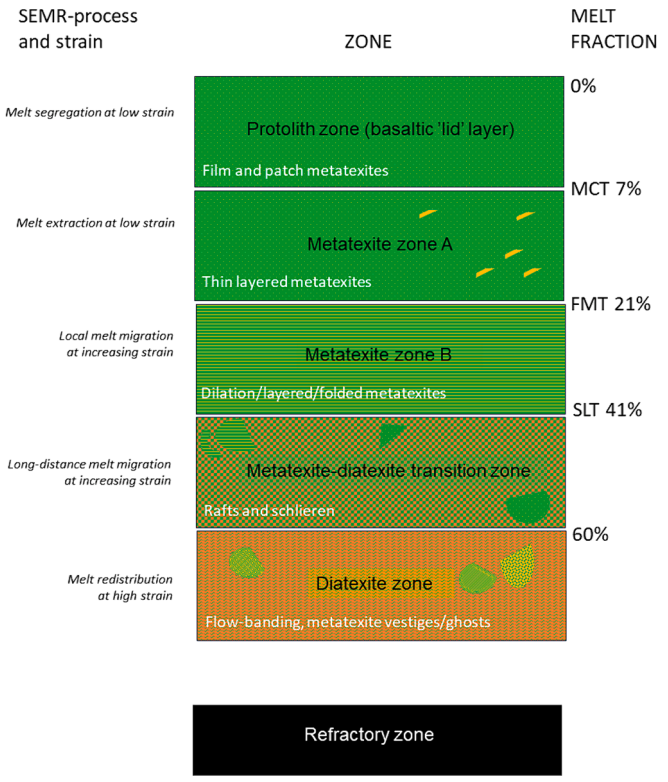

Fig. 11. Hypothetical illustration (not in scale) of the migmatite formation in terms of metabasalt strength drops (Chen et al., 2017; Zhang et al., 2019), see text for explanation.

structures are gently dipping, which is consistent with extensive lateral melt migration.

6.4. Constraints on the Archean tectonics

Any tectonic model suggested for the formation of the Lake Inari and analogue Archaean migmatitic TTG terrains, also known broadly as 'grey gneisses' or 'banded gneisses', should be able to explain the following observations:

- *Long duration of magmatism.* Geochronology of the Lake Inari and Lewisian gneiss terrains (Taylor et al., 2019; Joshi et al., 2024) suggests that melt persisted in the Archaean mid to lower crust for more than 250 m.y. pointing to more stagnant tectonics compared with present-day plate tectonics.
- *Existence of large migmatite terrains.* The Lake Inari terrain represents a flowing mass of diatexite melt and lacks plutonic boundaries.
- *Formation under variable synanatectic strain.* The migmatite structures formed in response to variable stresses and melt fractions during partial melting that caused changes in crustal rheology.
- *Abundant metabasalt rafts showing geochemical features similar to Phanerozoic oceanic hotspot-related suites.* These rafts might represent the remnants of an oceanic flood basalt layer disaggregated by partial melts.
- *Two geochemical TTG endmembers persisted from Eoarchaean to Neoarchaean.* The concentrations of garnet-compatible elements Y, Sc, Zn and Co in low-HREE TTGs are low, whereas in high-HREE TTGs they are high.
- *Controversy in the lack of garnet signature in metabasalt rafts while HREE TTGs show apparent garnet-control.* This could be explained by TTG melts flowing from sources that have undergone different paths of differentiation.
- *The structures pointing to 1) melt SEMR processes, 2) crystal mush flow and 3) disaggregation and assimilation of metabasalts. This can be explained by large-scale migmatization of a basaltic source.*

The simultaneous formation of low- and high-HREE TTGs points to a co-magmatic origin by processes such as mingling of magmas that have experienced different paths of differentiation or derive from compositionally diverse sources. Theoretically, a low-HREE pattern in TTGs may be inherited from a low-HREE composition of the protolith, or it can be formed because of residual garnet left in the source (Halla et al., 2009; Moyen, 2011), or due to amphibole fractionation from TTG magmas (Laurent et al., 2020). In the case of our samples, garnet-compatible elements Sc, Y, Zn and Co correlate with HREE, and we consider that TTG geochemistry is controlled by garnet rather than amphibole. Whether or not the garnet signature is related to the pressure conditions (i.e., depth of melting) of TTG formation (low-, medium-, and high-pressure TTGS of Moyen, 2011), fractionation of garnet during migmatization due to peritectic reactions (Kendrick and Yakymchuk, 2020) or involvement of garnet in the generation of basaltic protoliths (Heinonen et al., 2022; Hole et al., 2023) remains uncertain.

Nevertheless, we point out that numerous examples of plume-sourced large magma systems demonstrate wide ranges of HREE contents due to variable melting conditions and mantle source lithology (e.g. Haase et al., 2019; Heinonen et al., 2022; Tejada et al., 2023), so that protolith geochemistry is very likely to contribute to the HREE characteristics of TTGs. Furthermore, variably HREE-depleted basaltic units may well be spatially intercalated in such provinces, giving rise to plausible sources for geochemically diverse TTG suites.

Plumes are immense columns of superheated rocks rising from the mantle-core boundary. A widely supported model ascribes the formation of oceanic plateaus to extensive melting of starting plume heads, and the formation of oceanic island chains and associated submarine volcanoes to the melting of narrow plume stems (e.g., Richards et al., 1989). Based on the principle of uniformitarianism, we assume that since plumes exist today, it is highly likely that they also existed in the Archaean when the Earth was hotter. We further point out that whereas Earth's lithospheric plates are presently moving over plumes over time scales of millions of years, the stagnant-lid hypothesis for Archean Earth postulates restricted relative movement between plumes and the overlying lithosphere. A stationary hotspot environment would therefore allow the growth of a long-lived magmatically active oceanic plateau until the point where it breaks up by partial melting and weakening of the crust, leading to a prolonged formation of bimodal TTG-metabasalt association.

Recent studies of lithosphere above the Galápagos plume provide interesting additional constraints to hotspot environments. The detection of regionally extensive channels filled with volatile-rich low-degree melts at the base of the lithosphere (Naif et al., 2023) confirms that a plume may generate a long-living environment of hydrous melting in the deep lithosphere. We envisage a broadly plume-related setting to be a dynamically, thermally, and geochemically viable environment for generation of compositionally variable TTGs by partial melting of progressively thickening mafic crust over long-lived hotspot.

We maintain that the geochemistry of TTGs and metabasalts of Lake Inari is compatible with this scenario because the geochemical characteristics of Lake Inari metabasalts resemble those of Phanerozoic oceanic flood basalts. Following recent modelling of REE behavior during flood basalt magmatism (Heinonen et al., 2022), we postulate that variable melting conditions and possible lithological heterogeneity resulted in variable garnet-control during mantle melting. Specifically, Heinonen et al. (2022) demonstrated that steep oceanic island basalt-like HREE patterns can form beneath quite a thin lithosphere (~50 km) due to increased garnet stability in pyroxenite sources and that flat HREE patterns can form below thick lithosphere (~100 km) due to extensive melting of garnet peridotite.

We propose that melting of such variably HREE-depleted basaltic crust can explain the formation of low- and high-HREE TTGs by partial

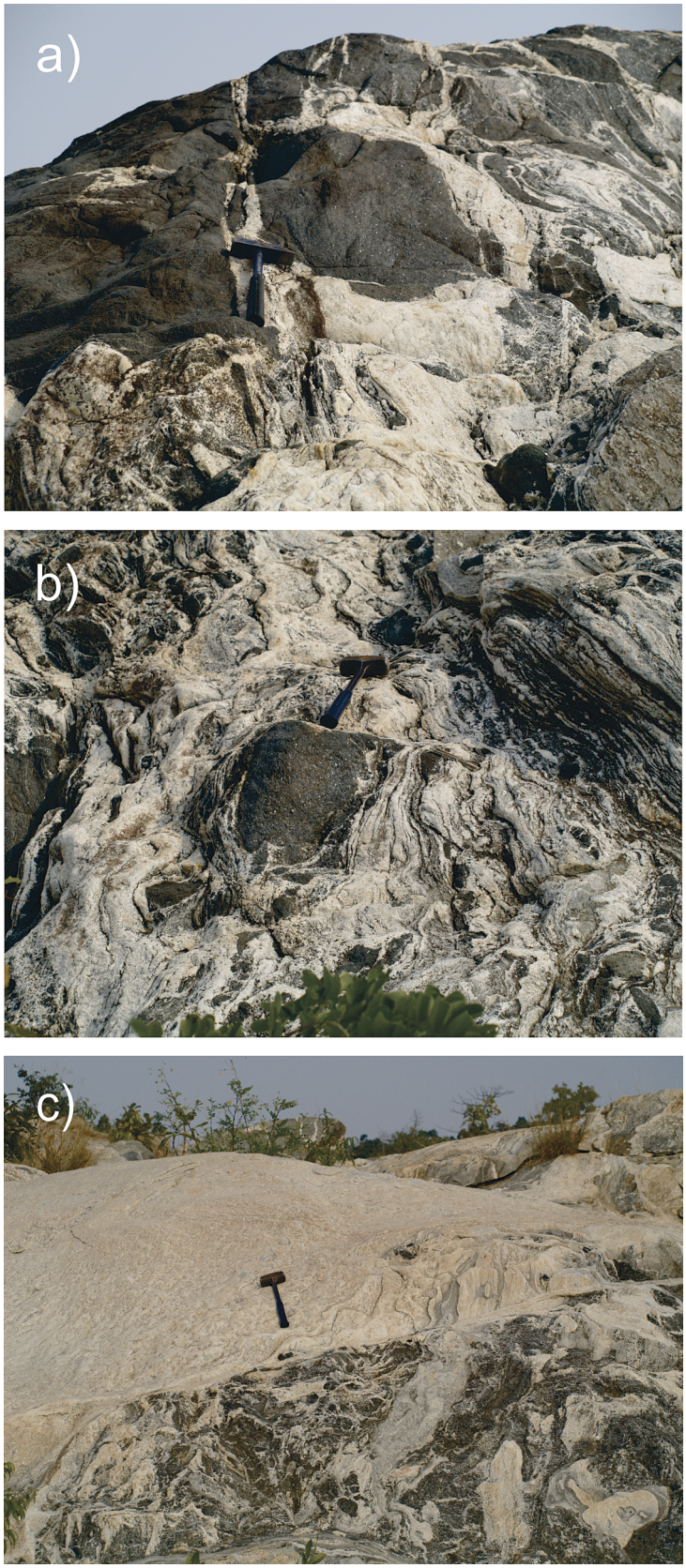

Fig. 12. Flowing diatexite melt breaks up amphibolite into diminishing rafts **(a)** that get variable morphology as tearing proceeds **(b)**. Accumulated metatexite melts produce leucocratic, residuum-free bodies **(c)**. Similar structures are common in the Lake Inari terrain. Photos from the Bhimakund waterfall, Singhbhum Craton, India.

melting of basalts. However, garnet may have been variably present also in the protolith of TTGs, and amphibole or garnet fractionation from TTG magmas could have been involved in the generation of the variable HREE patterns. We underscore that only rafts of a basaltic roof layer of the Inari protolith are exposed in the present level of erosion, which can explain the fact that all our metabasalt samples have high HREE compositions. Prolonged formation and partial melting of thick plateaus above a mantle plume may well be the mechanism that set off the evolution of continents, especially between 2.9 and 2.6 Ga. Their later accretion and rifting along with the development of the present-day plate tectonics led to their present-day configurations.

6.5. Conclusions

The Lake Inari terrain of the Lapland-Kola Province in northern Finland in Arctic Fennoscandia provides evidence for long-term migmatization of a plume-related basaltic plateau. The structures of the Lake Inari terrain have formed in different stages of migmatization processes. Overall, the terrain represents metatexite-diatexite transition and diatexite zones. Plateau basalts were converted to TTGs through migmatization, i.e. partial melt SEMR processes controlled by rheological crustal strength drops at different melt fractions and synanatectic strain.

(1) The Lake Inari amphibolites are low-magnesium and low-titanium subalkaline basalts metamorphosed in the upper amphibolite facies. They are geochemically markedly different from most rocks in continental and subduction settings and are most similar to oceanic hotspot-related suites.
(2) The two coeval and intermingled geochemical endmembers of TTGs, the low- and high-HREE types, differ especially in their garnet-compatible element (HREE, Mg, Sc, Y, Co and Zn) contents. The observed geochemical fingerprint may be inherited from a geochemically heterogeneous basaltic source.
(3) The bimodal TTG-metabasalt association shows various migmatite structures such as metatexites, metatexite-diatexite transitions and massive diatexites that have formed in response to rheological crustal strength drops, melt segregation, extraction, migration, and redistribution processes, and synanatectic strain.
(4) The Lake Inari terrain was a melt-rich crustal horizon formed by prolonged widespread migmatization of a basaltic plateau above a mantle plume at stagnant to sluggish lid tectonic setting.

CRediT authorship contribution statement

Jaana Halla: Writing – review & editing, Writing – original draft, Visualization, Resources, Project administration, Investigation, Funding acquisition, Conceptualization. **Kumar Batuk Joshi:** Writing – original draft, Visualization, Investigation, Conceptualization. **Arto Luttinen:** Writing – review & editing, Writing – original draft, Visualization, Conceptualization. **Esa Heilimo:** Writing – original draft, Investigation, Conceptualization. **Matti Kurhila:** Writing – original draft, Investigation, Data curation, Conceptualization.

Declaration of competing interest

The authors declare the following financial interests/personal relationships which may be considered as potential competing interests: Editorial membership for Precambrian Research, no involvement in the editorial review or the decision to publish this article, J.H. If there are other authors, they declare that they have no known competing financial interests or personal relationships that could have appeared to influence the work reported in this paper.

Data availability

The data is available online as supplementary material of this paper

Acknowledgements

We greatly acknowledge the support from the Geological Survey of Finland and funding from the K.H. Renlund foundation. We are thankful to Pentti Hölttä, the father of the idea to study the Lake Inari area, for his encouragement to take the action in the field. We express our especially warm thanks to Janne Henttunen (1975–2010), who was a warm-hearted and helpful young fisherman of the Lake Inari. Knowing the lake like the back of his hand, he helped us with navigation and worried about of our safety in sometimes harsh boating conditions on the lake during our very first field work periods. We are most grateful for Pekka Kivimäki whose excellent skills in skippering the boat, maintaining the research camp, sampling outcrops, and photographing the research material made this project possible. Anja Arkonsuo is warmly thanked for her invaluable role in the field work and petrographic investigations. We are also thankful for Satu and Ville Kurunsaari for kindly taking care of our boating and camping logistics, which enabled our latest visit to the research area in summer 2023. We thank two anonymous reviewers who helped us to crystallize our thoughts and significantly improve this manuscript. Finally, we are grateful for the Kilpisjärvi Biological Sation for providing a splendid environment for discussions and writing in Finnish Lapland.

Appendix A. Supplementary data

Supplementary data to this article can be found online at https://doi.org/10.1016/j.precamres.2024.107407.

References

Arndt, N., 2023. How did the continental crust form: No basalt, no water, no granite. Precambrian Research 397, 107196. https://doi.org/10.1016/j.precamres.2023.107196.

Barker, F., Arth, J.G., 1976. Generation of trondhjemite–tonalite liquids and Archean trondhjemite–basalt suites. Geology 4, 596–600. https://doi.org/10.1130/0091-7613(1976)4<596:GOTLAA>2.0.CO;2.

Bédard, J.H., 2018. Stagnant lids and mantle overturns: Implications for Archaean tectonics, magmagenesis, crustal growth, mantle evolution, and the start of plate tectonics. Geoscience Frontiers 9, 19–49. https://doi.org/10.1016/j.gsf.2017.01.005.

Chassé, M., Griffin, W.L., Alard, O., O'Reilly, S.Y., Calas, G., 2018. Insights into the mantle geochemistry of scandium from a meta-analysis of garnet data. Lithos 310–311, 409–421. https://doi.org/10.1016/j.lithos.2018.03.026.

Chen, Z., Liu, Y.-J., Chen, G.-N., Peng, Z.-L., 2017. Rheological transitions in progressive melting of rock and their geological constraints from the Fuhu metatexite-diatexite profile in Guangdong Province, SE China. Journal of Asian Earth Sciences 139, 192–201. https://doi.org/10.1016/j.jseaes.2017.02.009.

Chen, S.-S., Liu, J.-Q., Gao, R., Wang, Z.-W., 2021. Geochemistry of Cretaceous basalts from the Ontong Java Plateau: Implications for the off-axis plume–ridge interaction. Chemical Geology 564, 119815. https://doi.org/10.1016/j.chemgeo.2020.119815.

Chowdhury, P., Mulder, J.A., Cawood, P.A., Mukherjee, S., 2021. Magmatic thickening of crust in non-plate tectonic settings initiated the subaerial rise of Earth's first continents 3.3 to 3.2 billion years ago. Earth, Atmospheric, and Planetary Sciences 118 (46). https://doi.org/10.1073/pnas.2105746118 e2105746118.

Copley, A., Weller, O.W., 2024. Modern-style continental tectonics since the early Archean. Precambrian Research 403, 107324. https://doi.org/10.1016/j.precamres.2024.107324.

Cruden A.R., Weinberg, R.F., 2018. Chapter 2 - Mechanisms of Magma Transport and Storage in the Lower and Middle Crust—Magma Segregation, Ascent and Emplacement, in: Burchardt, S. (Ed.), Volcanic and Igneous Plumbing Systems, Elsevier, 13–53. DOI: 10.1016/B978-0-12-809749-6.00002-9.

Debon, F., Le Fort, P., 1983. A Chemical-Mineralogical Classification of Common Plutonic Rocks and Associations. Transactions of the Royal Society of Edinburgh: Earth Sciences 73, 135–149. https://doi.org/10.1017/S0263593300010117.

Garde, A.A., Windley, B.F., Kokfelt, T.F., Keulen, N., 2020. Archaean Plate Tectonics in the North Atlantic Craton of West Greenland Revealed by Well-Exposed Horizontal Crustal Tectonics, Island Arcs and Tonalite-Trondhjemite-Granodiorite Complexes. Frontiers of Earth Sciences 8, 540997. https://doi.org/10.3389/feart.2020.540997.

Haase, K.M., Regelous, M., Schöbel, S., Günther, T., de Wall, H., 2019. Variation of melting processes and magma sources of the early Deccan flood basalts, Malwa Plateau. India. Earth and Planetary Science Letters 524, 115711. https://doi.org/10.1016/j.epsl.2019.115711.

Halla, J., 2018. Highlights on Geochemical Changes in Archaean Granitoids and Their Implications for Early Earth Geodynamics. Geosciences 8 (9), 353. https://doi.org/10.3390/geosciences8090353.

Halla, J., 2020. The TTG-Amphibolite Terrains of Arctic Fennoscandia: Infinite Networks of Amphibolite Metatexite-Diatexite Transitions. Frontiers in Earth Sciences 8, 252. https://doi.org/10.3389/feart.2020.00252.

Halla, J., van Hunen, J., Heilimo, E., Hölttä, P., 2009. Geochemical and numerical constraints on Neoarchean plate tectonics. Precambrian Research 174, 155–162. https://doi.org/10.1016/j.precamres.2009.07.008.

Heilimo, E., Halla, J., Lauri, L.S., Rämö, O.T., Huhma, H., Kurhila, M.I., Front, K., 2009. The Paleoproterozoic Nattanen-type granites in northern Finland and vicinity – a postcollisional oxidized A-type suite. Bulletin of the Geological Society of Finland 81, 7–36. https://doi.org/10.17741/bgsf/81.1.001.

Heilimo, E., Elburg, M., Andersen, T., 2014. Crustal growth and reworking during Lapland-Kola orogeny in northern Fennoscandia: U-Pb and Lu-Hf data from the Nattanen and Litsa-Aragub-type granites. Lithos 205, 112–126. https://doi.org/10.1016/j.lithos.2014.06.014.

Hole, M.J., Pugsley, J.H., Jolley, D.W., Millett, J.M., 2023. Fractional crystallization of garnet in alkali basalts at >1.8 GPa and implications for geochemical diversity of Large Igneous Provinces. Lithos 460–461, 107397. https://doi.org/10.1016/j.lithos.2023.107397.

Hollocher, K., Robinson, P., Walsh, E., Roberts, D., 2012. Geochemistry of amphibolite-facies volcanics and gabbros of the Støren Nappe in extensions west and southwest of Trondheim, western gneiss region, Norway: A key to correlations and paleotectonic settings. American Journal of Science 312 (4), 357–416. https://doi.org/10.2475/04.2012.01.

Huang, G., Palin, R., Wang, D., Guo, J., 2020. Open-system fractional melting of Archean basalts: implications for tonalite–trondhjemite–granodiorite (TTG) magma genesis. Contributions to Mineralogy and Petrology 175, 102. https://doi.org/10.1007/s00410-020-01742-9.

Huhma, H., 2019. Isotope results from Lapland-Kola Province in Finland. Geological Survey of Finland, Open File Research Report 37. https://tupa.gtk.fi/raportti/arkisto/37_2019.pdf.

Jackson, M.G., Hart, S.R., Koppers, A.A.P., Staudigel, H., Konter, J., Blusztajn, J., Kurz, M., Russell, J.A., 2007. The return of subducted continental crust in Samoan lavas. Nature 448, 684–687. https://doi.org/10.1038/nature06048.

Johnson, T.E., Kirkland, C.L., Gardiner, N.J., Brown, M., Smithies, R.H., Santosh, M., 2019. Secular change in TTG compositions: Implications for the evolution of Archaean geodynamics. Earth and Planetary Science Letters 505, 65–75. https://doi.org/10.1016/j.epsl.2018.10.022.

Joshi, K.B., Banerji, U.S., Dubey, C.P., Oliveira, E.P., 2022. Detrital Zircons in Crustal Evolution: A Perspective from the Indian Subcontinent. Lithosphere (special 8), 3099822. https://doi.org/10.2113/2022/3099822.

Joshi, K.B., Bhattacharjee, J., Rai, G., Halla, J., Ahmad, T., Kurhila, M., Heilimo, E., Choudhary, A.K., 2017. The diversification of granitoids and plate tectonic implications at the Archaean-Proterozoic boundary in the Bundelkhand craton, Central India. In: Halla, J., Whitehouse, M., Ahmad, T. & Bagai, Z., (eds) Archaean Cratons: Crust–Mantle Interactions and Granitoid Diversification: Insights from Archaean Cratons. Geological Society, London, Special Publications, 449, 123–157. DOI: 10.1144/SP449.8.

Joshi, K.B., Halla, J., Kurhila, M., Heilimo, E., 2024. Prolonged parallel chronology of distinct TTG types in the Lake Inari terrain, Arctic Fennoscandia: Implications for a stationary plume-related source. Precambrian Research (In press).

Karinen, T., Lepistö, S., Konnunaho, J., Lauri, L. S., Manninen, T., and Huhma, H., 2015. Unit Description Report, Enontekiö, Käsivarsi. Finnish: Yksikkökuvausraportti, Enontekiö, Käsivarsi. Rovaniemi: Geological Survey of Finland. https://tupa.gtk.fi/raportti/arkisto/66_2015.pdf.

Kendrick, J., Yakymchuk, C., 2020. Garnet fractionation, progressive melt loss and bulk composition variations in anatectic metabasites: Complications for interpreting the geodynamic significance of TTGs. Geoscience Frontiers 11, 745–763. https://doi.org/10.1016/j.gsf.2019.12.001.

Kendrick, J., Duguet, M., Yakymchuk, C., 2021. Diversification of Archean tonalite-trondhjemite-granodiorite suites in a mushy middle crust. Geology 50, 76–80. https://doi.org/10.1130/G49287.1.

Kinney, C., Kendrick, J., Duguet, M., Yakymchuk, C., 2023. Redistribution of heat-producing elements during melting of Archean crust. Journal of Metamorphic Geology 42, 197–224. https://doi.org/10.1111/jmg.12751.

Kujansuu, R., Eriksson, B., Grönlund, T., 1998. Lake Inarijärvi, northern Finland: Sedimentation and Quaternary evolution. Tutkimusraportti - Geologian Tutkimuskeskus 143, 1–25. https://tupa.gtk.fi/julkaisu/tutkimusraportti/tr_143.pdf.

Kusky, T., Windley, B.F., Polat, A., Wang, L., Ning, W., Zhong, Y., 2021. Archean dome-and-basin style structures form during growth and death of intraoceanic and continental margin arcs in accretionary orogens. Earth-Science Reviews 220, 103725. https://doi.org/10.1016/j.earscirev.2021.103725.

Lahtinen, R., Huhma, H., 2019. A revised geodynamic model for the Lapland-Kola orogen. Precambrian Research 330, 1–19. https://doi.org/10.1016/j.precamres.2019.04.022.

Laurent, O., Martin, H., Moyen, J.F., Doucelance, R., 2014. The diversity and evolution of late-Archean granitoids: Evidence for the onset of "modern-style" plate tectonics between 3.0-2.5 Ga. Lithos 205, 208–235. https://doi.org/10.1016/j.lithos.2014.06.012.

Laurent, O., Vander Auwera, J., Bingen, B., Bolle, O., Gerdes, A., 2019. Building up the first continents: mesoarchean to paleoproterozoic crustal evolution in West Troms, Norway, inferred from granitoid petrology, geochemistry and zircon U-Pb/Lu-Hf isotopes. Precambrian Research 321, 303–327. https://doi.org/10.1016/j.precamres.2018.12.020.

Laurent, O., Björnsen, J., Wotzlaw, J.-F., Bretscher, S., Silva, M.P., Moyen, J.-F., Ulmer, P., Bachmann, O., 2020. Earth's earliest granitoids are crystal-rich magma reservoirs tapped by silicic eruptions. Nature Geoscience 13, 163–169. https://doi.org/10.1038/s41561-019-0520-6.

Liou, P., Guo, J., 2019. Generation of Archaean TTG gneisses through amphibole-dominated fractionation. Journal of Geophysical Research: Solid Earth 124, 3605–3619. https://doi.org/10.1029/2018JB017024.

Liu, J., Liu, F., Ding, Z., Li, Y., Jin, W., Tian, Z., 2024. Mesoarchean-Neoarchean coupled crust–mantle differentiation followed by gravity-driven lithospheric delamination and subduction initiation in the North China Craton. Precambrian Research 404, 107349. https://doi.org/10.1016/j.precamres.2024.107349.

Mathieu, L., 2022. Modeling the chemical heterogeneity of tonalite-trondhjemite-granodiorite intrusive suites. Lithos 422–423. https://doi.org/10.1016/j.lithos.2022.106744.

McDonough, W.F., Sun, S.-S., 1995. The composition of the Earth. Chemical Geology 120, 223–253. https://doi.org/10.1016/0009-2541(94)00140-4.

Meriläinen, K., 1976. The granulite complex and adjacent rocks in Lapland, northern Finland. Bulletin of the Geological Society of Finland 289, 129 pp.

Mitra, A., Dey, S., 2017. Occurrence of Two Different Types of Paleoarchean TTGs in Singhbhum craton, Eastern India: Insight from Geochemistry and Zircon Saturation Thermometry. In Proceedings of the American Geophysical Union, Fall Meeting 2017, New Orleans, LA, USA, 11–15 December 2017.

Moyen, J.F., Martin, H., 2012. Forty years of TTG research. Lithos 148, 312–336. https://doi.org/10.1016/j.lithos.2012.06.010.

Moyen, J. F., 2011. The composite archaean grey gneisses: petrological significance, and evidence for a non-unique tectonic setting for archaean crustal growth. Lithos 123, 21–36. https://doi: 10.1016/j.lithos.2010.09.015.

Murphy, M.E., Macdonald, J.E., Fischer, S., Gardiner, N.J., White, R.W., Savage, P.S., 2024. Silicon isotopes in an Archaean migmatite confirm seawater silicification of TTG sources. Geochimica Et Cosmochimica Acta 368, 34–49. https://doi.org/10.1016/j.gca.2024.01.018.

Myhre, P.I., Corfu, F., Bergh S.G, Kullerud, K., 2013. U–Pb geochronology along an Archaean geotransect in the West Troms Basement Complex, North Norway. Norwegian Journal of Geology 93, 1–24. Trondheim.

Naif, S., Miller, N.C., Shillington, D.J., Bécel, A., Lizarralde, D., Bassett, D., Hemming, S. R., 2023. Episodic intraplate magmatism fed by a long-lived melt channel of distal plume origin. Science. Advances 9, eadd3761. https://doi.org/10.1126/sciadv.add3761.

Nutman, A.P., Friend, C.R.L., Bennett, V.C., 2024. Convergent plate boundary environments for formation of ≥3800 Ma mafic–ultramafic assemblages (Isua area, Greenland): Implications for early global geodynamics. Geoscience Frontiers 15 (3), 101794. https://doi.org/10.1016/j.gsf.2024.101794.

Palin, R.M., White, R.W., Green, E.C.R., 2016. Partial melting of metabasic rocks and the generation of tonalitic-trondhjemitic-granodioritic (TTG) crust in the Archaean: constraints from phase equilibrium modelling. Precambrian Research 287, 73–90. https://doi.org/10.1016/j.precamres.2016.11.001.

Patison, N. L., Korja, A., Lahtinen, R., Ojala, V. J., and the FIRE working Group, 2006. FIRE seismic reflection profiles 4, 4A and 4B: Insights into the Crustal Structure of Northern Finland from Ranua to Näätämö. Geological Survey of Finland, Special Paper 43, 161–222. https://tupa.gtk.fi/julkaisu/specialpaper/sp_043_pages_161_222.pdf.

Pearce, J.A., 2008. Geochemical fingerprinting of oceanic basalts with applications to ophiolite classification and the search for Archean oceanic crust. Lithos 100, 14–48. https://doi.org/10.1016/j.lithos.2007.06.016.

Pourteau, A., Doucet, L.S., Blereau, E.R., Volante, S., Johnson, T.E., Collins, W.J., Li, Z.-X., Champion, D.C., 2020. TTG generation by fluid-fluxed crustal melting: Direct evidence from the Proterozoic Georgetown Inlier, NE Australia. Earth and Planetary Science Letters 550, 116548. https://doi.org/10.1016/j.epsl.2020.116548.

Rapp, R.P., Watson, E.B., 1995. Dehydration Melting of Metabasalt at 8–32 kbar: Implications for Continental Growth and Crust-Mantle Recycling. Journal of Petrology 36, 891–931. https://doi.org/10.1093/petrology/36.4.891.

Richards, M.A., Duncan, R.A., Courtillot, V.E., 1989. Flood basalts and hot-spot tracks: plume heads and tails. Science 246 (4926), 103–107. https://doi.org/10.1126/science.246.4926.103.

Riis, F., 1996. Quantification of Cenozoic vertical movements of Scandinavia by correlation of morphological surfaces with offshore data. Global and Planetary Change 12, 331–357. https://doi.org/10.1016/0921-8181(95)00027-5.

Rollinson, H., 2021. Do all Archaean TTG rock compositions represent former melts? Precambrian Research 367, 106448. https://doi.org/10.1016/j.precamres.2021.106448.

Rollinson, H.R., 2023. The growth of the Zimbabwe craton during the Neoarchaean. Contribution to Mineralogy and Petrology 178, 1. https://doi.org/10.1007/s00410-022-01978-7.

Rosenberg, C.L., Handy, M.R., 2005. Experimental deformation of partially melted granite revisited: implications for the continental crust. Journal of Metamorphic Geology 23, 19–28. https://doi.org/10.1111/j.1525-1314.2005.00555.x.

Sawyer, E.W., 2008. Atlas of Migmatites, The Canadian Mineralogist, Special Publication 9. NRC Research Press, Ottawa, ON, p. 371.

Smit, M.A., Musiyachenko, K.A., Goumans, J., 2024. Archaean continental crust formed from mafic cumulates. Nature Communications 15, 692. https://doi.org/10.1038/s41467-024-44849-4.

Sun, S.S., McDonough, W.F., 1989. Chemical and isotopic systematics of oceanic basalts: implications for mantle composition and processes. In: Saunders A.D., Norry M.J.

(eds) Magmatism in the ocean basins. Geological Society of London Special Publication 42, 313–345. DOI: 10.1144/GSL.SP.1989.042.01.19.

Tarduno, J.A., Cottrell, R.D., Bono, R.K., Rayner, N., Davis, W.J., Zhou, T., Nimmo, F., Hofmann, A., Jodder, J., Ibañez-Mejia, M., Watkeys, M.K., Oda, H., Mitra, G., 2023. Hadaean to Palaeoarchaean stagnant-lid tectonics revealed by zircon magnetism. Nature 618, 531–536. https://doi.org/10.1038/s41586-023-06024-5.

Taylor, R.J.M., Johnson, T.E., Clark, C., Harrison, R.J., 2019. Persistence of melt-bearing Archean lower crust for >200 m.y. – An example from the Lewisian Complex, northwest Scotland. Geology DOI 10.17863/CAM.45763.

Tejada, M.L.G., Mahoney, J.J., Neal, C.R., Duncan, R.A., Petterson, M.G., 2002. Basement geochemistry and geochronology of Central Malaita, Solomon Islands, with implications for the origin and evolution of the Ontong Java Plateau. Journal of Petrology 43, 449–484. https://doi.org/10.1093/petrology/43.3.449.

Tejada, M.L.G., Sano, T., Hanyu, T., Koppers, A.A.P., Nakanishi, M., Miyazaki, T., Ishikawa, A., Tani, K., Shimizu, S., Shimizu, K., Vaglarov, B., Chang, Q., 2023. New evidence for the Ontong Java Nui hypothesis. Scientific Reports 13, 8486. https://doi.org/10.1038/s41598-023-33724-9.

Thompson, R., Gibson, S., Dickin, A., Smith, P., 2001. Early Cretaceous basalt and picrite dykes of the southern Etendeka region, NW Namibia: windows into the role of the Tristan mantle plume in Paraná-Etendeka magmatism. Journal of Petrology 42, 2049–2081. https://doi.org/10.1093/petrology/42.11.2049.

Vandenburg, E.D., Nebel, O., Smithies, H.R., Capitanio, F.A., Miller, L., Cawood, P.A., Millet, M.A., Bruand, E., Moyen, J.F., Wang, X., Nebel-Jacobsen, Y., 2023. Spatial and temporal control of Archean tectonomagmatic regimes. Earth-Science Reviews 241, 104417. https://doi.org/10.1016/j.earscirev.2023.104417.

Weinberg, R.F., Vernon, R.H., Schmeling, H., 2021. Processes in mushes and their role in the differentiation of granitic rocks. Earth-Science Reviews 220, 103665. https://doi.org/10.1016/j.earscirev.2021.103665.

Wu, Z., Zhao, G., 2022. Hydrous plumes in the Archean and the origin of continents. Science Bulletin 67, 2023–2025. https://doi.org/10.1016/j.scib.2022.09.016.

Wyman, D., 2018. Do cratons preserve evidence of stagnant lid tectonics? Geoscience Frontiers 9, 3–17. https://doi.org/10.1016/j.gsf.2017.02.001.

Xia, L.-Q., 2014. The geochemical criteria to distinguish continental basalts from arc related ones. Earth-Science Reviews 139, 195–212. https://doi.org/10.1016/j.earscirev.2014.09.006.

Xu, Y., Chung, S.-L., Jahn, B.-M., Wu, G., 2001. Petrologic and geochemical constraints on the petrogenesis of Permian-Triassic Emeishan flood basalts in southwestern China. Lithos 58, 145–168. https://doi.org/10.1016/S0024-4937(01)00055-X.

Zhang, J., Liu, W., Yakymchuk, C., Sa, R., Zheng, Z., Ding, R., Tang, G., Liu, H., Xu, Q., Wang, Y., 2019. Partial melting and Crustal Deformation during the Early Paleozoic Wuyi-Yunkai Orogeny: Insights from Zircon U-Pb Geochronology and Structural Analysis of the Fuhuling Migmatites in the Yunkai Region, South China. Minerals 2019, *9*(10), 621. DOI: 10.3390/min9100621.

Zhang, Y., Namur, O., Charlier, B., 2023. Experimental study of high-Ti and low-Ti basalts: liquid lines of descent and silicate liquid immiscibility in large igneous provinces. Contributions to Mineralogy and Petrology 178. https://doi.org/10.1007/s00410-022-01990-x.

Zhou, H. Hoernle, K, J., Geldmacher, J., Hauff, F., Homrighausen, S., Garbe-Schönberg, D., Jung, S., 2020. Geochemistry of Etendeka magmatism: Spatial heterogeneity in the Tristan-Gough plume head. Earth and Planetary Science Letters 535, 116123. DOI: 10.1016/j.epsl.2020.116123.